

Optical Characterization and Properties of Polymeric Materials for Optoelectronic and Photonic Applications

A. N. Alias

Z. M. Zabidi

A.M.M. Ali

M. K. Harun

Faculty of Applied Sciences, Universiti Teknologi MARA
40450 Shah Alam, Selangor D.E
Malaysia

M.Z.A. Yahya

Faculty of Science & Defence Technology, Universiti Pertahanan Nasional Malaysia,
Kemsg. Besi, 57000 Kuala Lumpur
Malaysia

Abstract

The optical properties of polymers attract considerable attention because of their potential optoelectronic applications, such as in polymer-based light-emitting diodes, light electrochemical cells, and solar cells. To optimize the performance of optoelectronic and photonic devices, some polymers are modified through the introduction of specific end groups, copolymerization, grafting, crosslinking, blending, and hybridization with other inorganic polymers. All these techniques affect the optical properties of the polymer. This paper reviews the fundamental emission and optical properties, such as absorption, reflection, and polarization effect, of numerous polymer materials. These aspects are important to be considered in optoelectronic devices.

Introduction

Polymers are widely used in electrical and electronic applications. In early works, polymers have been used as insulators because of their high resistivity and dielectric properties. Polymer-based insulators are used in electrical equipment to separate electrical conductors without passing current through themselves. The insulator applications of polymers include printed circuit boards, wire encapsulants, corrosion protective electronic devices, and cable sheathing materials [1]. Polymers have several advantages, such as easy processing, low cost, flexibility, high strength, and good mechanical properties. In the microelectronic fabrication industry, polymers are used in the photolithography process.

In 1977, Shirakawa et al. [2], macdiarmid [3], and Heeger[2]found that the conducting polymer polyacetylene can be used as a dopant and change the conductivity of the doped material. Since this discovery, polymers have been extensively studied as new materials for electronic and optoelectronic applications. To enhance the conductivity using polymers as well as to create new optical and electrical properties of polymer, four process of doping have been identified, including chemical doping, photochemical doping, electrochemical doping, and interfacial doping [3, 4]. Optoelectronic and electronic materials are gaining interest because of their implementation of various functions of light, such as modulation, generation, switching, and detection in the optical waveguide structure formed on the substrate [5]. Polymers can become suitable materials for optoelectronic and photonic applications.

Much progress has been made in understanding the fundamental physical and chemical properties of optoelectronic and photonic devices to optimize device efficiency. However, the correlation between the physical and chemical properties is not fully understood. One of the most important characteristics is the optical properties. Optical characterizations of polymer such as optical absorption, luminescence spectra, infrared dichroism, and Raman polarization are the most vital tools used to examine the electronic properties of polymers [6-8].

These techniques rely on the transition of electrons from the highest occupied molecular orbital (HOMO) to the lowest unoccupied molecular orbital (LUMO) or the nonlinear optical properties of polymeric material. To optimize the performance of optoelectronic and photonic devices, polymers are modified through the introduction of specific end groups, copolymerization, grafting, crosslinking, blending, and hybridization with other inorganic polymers. In copolymers, the monomeric unit may be arranged randomly, alternating, blocked, or grafted. Another polymer can be joined with other polymers by crosslinking.

Polymer blending is the simplest, most well-known technique in polymer engineering for creating new solid materials with more enhanced properties than homopolymers. Polymer blending with other polymer materials or small molecules such as anthracene, pyrene, or pyridine has been performed [9]. Polymer materials have also been mixed with other salts or hybridized with other inorganic/nanoparticle materials to modify the optical and electrical properties of the polymer system. All these techniques affect the optical properties of polymers. This review is aimed to understand the fundamental optical properties of polymer materials widely used in optoelectronic and photonic applications. In section 2, we review the basic device operation and polymeric material which has been used in optoelectronic and photonic devices.

While in section 3, experimental and physical description to characterize the optical parameter in polymeric material. The optical properties such as optical absorption band, dispersion behavior, anisotropic, excitation and emission spectra have been explained in section 4. The effect of conjugation length in Raman Spectra also has been discussed in same section. By knowing the fundamental optical properties of polymers, we believe that devices operation can be improved and further developments can be made. The studied optical properties of polymer materials include absorption, reflection, and emission properties, as well as basic optoelectronic device operation.

Polymeric Material and Basic Operation in Optoelectronic and Photonic Devices

Polymer Light-Emitting Diodes (PLEDs)

In 1987, Tang from Kodak reported low-voltage organic light-emitting diodes (LEDs) [10]. Three years later, Burroughes invented the first PLEDs using poly(phenylenevinylene) (PPV) [11]. Since then, research on PLEDs has rapidly grown. Basically, PLEDs consist of a hole transport layer (HTL) and an electron transport layer (ETL) sandwiched by an anode and a cathode. Adachi proposed that materials for the HTL must have the abilities to facilitate a low driving voltage, block the electron passing through the emission layer which is known as electron blocking layer, and prevent quenching molecular exciton [12]. For single HTL/EBL, aromatic amine derivative has widely been used and it shows good thermal stability [13].

Non-conjugated polymers such as polyaniline (PANI) and polycarbazole (PVK) have also been identified to be suitable candidates for HTL/EBL [14, 15]. Currently, deoxyribonucleic acid (DNA) has been used as EBL in PLED application or known as bioLED. The luminescence efficiency is higher in LED using DNA as EBL compared to PVK and poly(methyl methacrylate) (PMMA) [16]. DNA used in EBL is normally extracted from salmon sperm DNA to perform DNA complex. The multilayer bioLED made from tris-(8-hydroxyquinoline) aluminum (Alq_3) as the emitting layer shows low turn-on voltage ($\sim 5V$), high efficiency, high brightness and also good white color stability [17]. Madhwal et al. reported that salmon DNA as EBL also enhances the performance of poly[2-methoxy-5-(2'-ethylhexyloxy)-1,4-phenylenevinylene] (MEH-PPV) and poly[9,9-dioctylfluorene] (PFO)-based light emitting diode [18].

They also proposed that EBL made from DNA has high potential barrier which could trap electron injected from cathode. The recombination with hole injected from anode could produce high luminescence intensity. On the other hand, the ETL materials must have excellent ETL and exciton confinement [19]. When voltage is applied to the anode, holes are injected to the HTL and electrons are injected to the ETL, as shown in Figure 1. To ensure that the charge carriers are effectively injected, the anode must have a high work function and fit with the HOMO HTL and vice versa at the cathode [20, 21]. The carriers are injected either through the Fowler-Nordheim tunneling mechanism or Schottky thermionic emission [22]. Electrons and holes migrate apart from the electrode to form excitons at the polymer emitting layer. The emitting layer for confining the exciton is the key factor for color emission in PLED. The suitable material for emitting layer must consist of conjugated π -bonding.

This material can be small molecule oligomer which known as small molecule light emitting diode (SMOLED) or polymer molecule-based PLED. In fabrication process, since small molecule has poor solubility, therefore vacuum vapor deposition technique is the best choice to fabricate SMOLED. While, PLED can be fabricated by solution process namely spin coating or ink-jet printing which are suitable for low cost and wide area display application. Devices-based multilayer structure SMOLED are more complexes and sophisticated architecture compared to the PLED which it depends on the molecular energy gap alignment [23]. There are two types of exciton based on the quantum number, namely, singlet and triplet excitons.

Normally, triplet excitons tend to undergo non-radiative recombination, which results in joule heating in plds [24]. To avoid this phenomenon, organic ligands such bis[2-(2'-benzothienyl)-

Pyridinaton, C^{3+} iridium (acetylacetonate) have been used to transfer the triplet state to the f level of Ir and generate electro phosphorescence[25]. For electro phosphorescence light emitting diode, phosphorescence SMOLED has shown a higher efficiency compared to the phosphorescence PLED[26]. In order to have both advantages from SMOLED and PLED, a hybrid LED has been developed to enhance the stability and efficiency of the device.

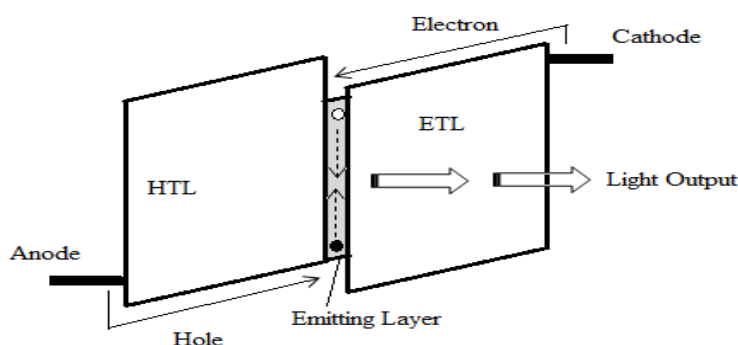


Figure 1: Schematic of PLED

The choosing of an anode material is very important in fabricating PLED. The material should have high work function to ensure the hole can be injected into the organic material. Besides that, the anode must also be a good transparence conducting material for its application in photovoltaic and emitting-based devices. It is well known that in OLED and PLED, it has widely been used as the transparent conducting electrode. Tang and Van Slayke[10] were constructed the first novel electroluminescent device by using ITO as the electrode. Research done by Zhu et al. [27] showed that ITO thin film was 80% transparent especially for visible light. A research group from Princeton University [28] also used 70% transparence ITO in the top and low contact of their device. The driving voltage of PLED also depends on the electrode resistance and has higher turn-on voltage when the electrode resistance is higher[28].

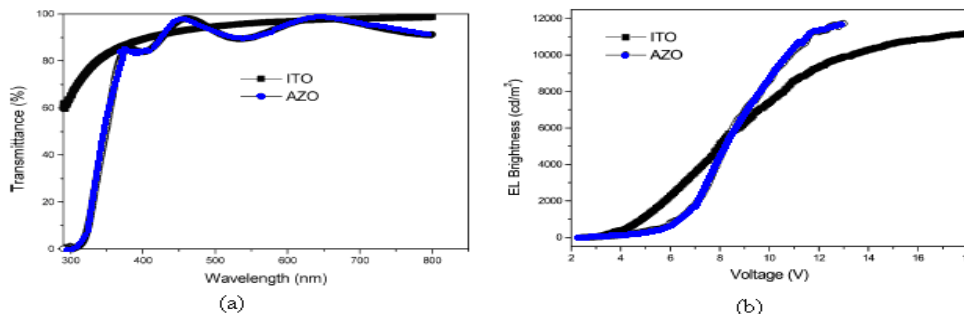


Figure 2. (a) the transmission spectrum for ITO and AZO (b) brightness in PLED by using ITO and AZO as the anode[29]. Reprinted from Physics Letters A, Vol 346, Denghui Xu, Zhenbo Deng, Ying Xu, Jing Xiao, Chunjun Liang, Zhiliang Pei, Chao Sun, *An Anode with Aluminum Doped on Zinc oxide thin Films For Organic light emitting devices*, Pages 148–152, Copyright (2005), with permission from Elsevier.

Beside ITO, aluminum doped zinc oxide (AZO) has also been used as the anode. If small amount of aluminum is doped, ZnO can tune the conductivity from an n-type to a p-type semiconductor. AZO has a potential to replace ITO because it is less expensive and non-toxic compared to the ITO. The difference in brightness performances of OLED spectrum transmission between AZO and ITO can be shown in Figure 2 [29]. The contamination of AZO in the organic material is lower than that of ITO. This is because in ITO, the diffusion of indium is easier to occur and hence contaminates the active layer of OLED [21]. However, thin film stability has still become the main issue in AZO.

Polymer Light-Emitting Electrochemical Cells (lecs)

Another type of electroluminescence polymer is lecs. The operating mechanism of polymer lecs differs from the two other important organic/polymer electroluminescent devices, namely LEDs and electrochemiluminescent (ECL) cells. In polymer lecs, the active layer consists of a luminescence polymer blend with a polymer electrolyte and an ionic salt. When voltage is applied to the active layer, the charge is injected to the luminescence polymer. At the anode, the luminescence polymer begins to oxidize; at the cathode, the reduction process occurs (Figure 3). The counterions from the electrolyte begin to redistribute near the electrode interface to compensate for the charges exchanged during the oxidation and reduction of the luminescence polymer [30]. Then, electrochemical p- and n-doped regions are created.

Once the junctions are formed, carrier recombination occurs in the active layer region. The movement of ions is slow and depends on the ionic conductivity of the film. The ions also move during the transient junction formation [31]. However, the luminescence of ECL devices is based on the recombination caused by excited redox species. Given the conjugate polymers in the p- and n-doped regions, lecs make ohmic contact with one another. An optical beam induced current is used to confirm the p and n doping [32]. The minimum voltage (turn-on voltage) to form in situ p-n junction is given by Eq. (1)

$$V = \frac{E_g}{q} \quad (1)$$

Where E_g is the energy gap of the conjugate polymer and q is the elementary charge. The active layer LEC must have reversible oxidation and reduction within the potential window of electrochemical stability [33]. The current on lecs consists of two components: an electronic contribution and an ionic contribution. Theoretical calculations have shown that the junction in lecs consists of either a graded junction or two doped layers separated by an inner region of depleted ions (p-i-n junction) [34]. The injected electrons and holes recombine and emit light from the insulating region, as shown in Figure 2. LeCs have higher electroluminescence quantum efficiency than LEDs. LeCs also display a lower operating voltage (<4 V) and a higher power efficiency than LEDs [35, 36].

However, de Mello et al. proposed that the distribution of ionic space charges in the active layer cancels the internal electric field and lowers the injection barriers [37]. They also suggested that Schottky contacts form between a metal and a luminescence polymer. The distribution of ionic charges near the contact renders lecs insensitive to the cathode or anode work function. Meanwhile, Reiss suggested that the LEC transport properties are similar to those of mixed ionic electronic conductors based on Galvanic cells [38, 39].

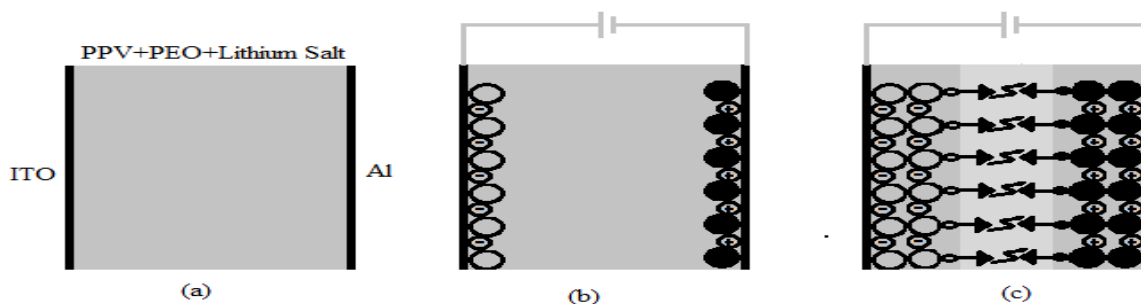


Figure 3: (a) PPV blend with polymer electrolyte and salt. (b) Oxidation and reduction process in LEC. (c) Recombination process. Redrawn and adapted from reference [30].

Solar Cells

For the past decade, the active materials used for the fabrication of solar cells are mainly inorganic materials, such as silicon (Si), gallium-arsenide (GaAs), cadmium-telluride (CdTe), and cadmium-indium-selenide. Amorphous silicon, CdTe, and CIGS are more recent thin-film technologies in solar cells. Solar cells based on silicon account for over 85% of all solar cells [40]. Even when the production costs can be reduced, the large-scale production of current silicon solar cells is limited by the deficit of some components required, e.g., solar-grade silicon. Photovoltaic hardly contribute to the energy market because they are too expensive [41]. An alternative is the introduction of organic photovoltaic such as conjugate polymers [42, 43]. Although organic photovoltaics exhibit lower power conversion efficiency than inorganic solar cells [44-46], they have the advantages of mechanical flexibility [47], material stability [48], low cost, and large-scale fabrication [49, 50].

The basic idea of photovoltaic devices is that the atoms in a semiconductor placed under sunlight absorb photons from the solar radiation. If these photons are of sufficiently high energy, an electron in the valence band (also known as the HOMO) uses the absorbed energy to move up to the conduction band of the semiconductor (also known as the LUMO), thereby forming an exciton. Exciton dissociation then follows. The electrons are collected at the cathode (such as aluminum), whereas holes are collected at the anode (such as ITO). This process enables electrons to move freely through the semiconductor to an electrical contact, from where it is driven by a small voltage through wires as current. Figure 4 shows the schematic of photocurrent process in solar cells.

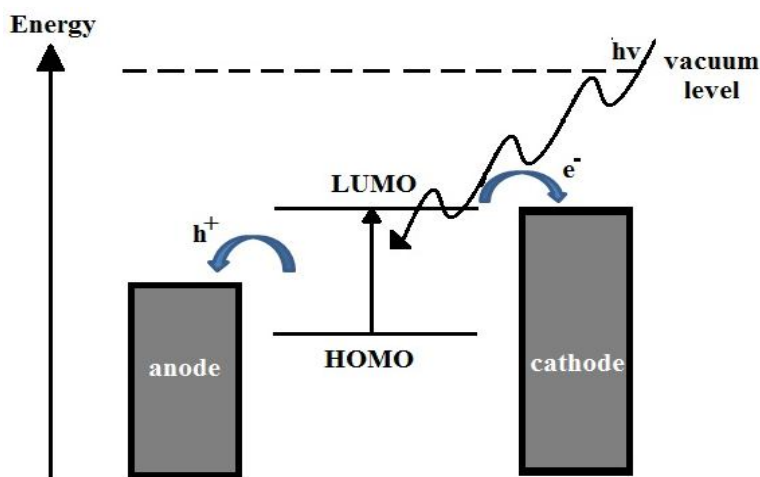


Figure 4: Schematic of photocurrent process in solar cells.

Nowadays, nanostructured materials became promising candidates that could provide a large area and high efficiency of solar cells. Third generation solar cells compose of quantum dot (QD). The absorption of light in QD produces multiple hole-electron pairs which are known as multiple exciton generation, and thus generate photocurrent in polymeric solar cells. There are three types of QD solar cell configuration namely quantum dot arrays in p-i-n cells, quantum dot dye-sensitized solar cells (DSSC) and quantum dot dispersed in polymer solar cell. For the type of QD arrays in p-i-n cell, quantum dots are arranged in inter-quantum dot spacing which create electronic coupling, and thus minibands are formed to allow quantum transport in intrinsic region [51].

In the case of QD dye-sensitized solar cells (DSSCs), they consist of liquid electrolyte blended with an absorbance molecule. In DSSCs, electrons in dye molecules are transferred to a wide bandgap nanocrystalline material such as TiO_2 , ZnO and Nb_2O_5 [52, 53]. A redox reaction occurs in the dye and polymer electrolyte system, and thus produces electron migration through the external load. Meanwhile, solar cells configuration on QD dispersed in polymer matrix composes of conducting polymer such as MEH-PPV [54], Poly[2-methoxy-5-(3,7-dimethyloctyloxy)-1,4-phenylenevinylene] (MDMO-PPV) [55] and P3HT [56]. Upon light absorption, the carriers remain in QD and collected through diffusion and percolation in nanocrystalline phase to an electric contact to QD network [57].

Experimental Instrument for Optical Characterization

The successful optical characterization of polymers requires careful sample preparation, attention to experiment details, and cautious handling instrument. Given that optical characterizations are highly sensitive to impurities and environmental conditions, serious precaution is required in handling samples. Careful baseline correction is also required to ensure data reliability.

UV-vis Absorption

Absorption spectroscopy is a technique wherein the absorption of electromagnetic wave is measured as a function of the frequency or wavelength. The absorption process induces an interaction between electromagnetism and the sample, which can be interpreted through variations in the absorption spectra. An absorption spectrum is a fingerprint of a molecule or polymer material. UV-vis absorption is a commonly used analytical tool for studying the interactions between electrons and radiation. On the other hand, infrared absorption is widely used to analyze the interactions between the vibration energy of bonds and electromagnetic waves.

Literature on the instrumentation and technical aspects of absorption spectroscopy is extensive [58-60]. We conclude that there are four basic components, namely, the light source, monochromator, sample holder, and optical detector. In general, optical absorption spectrophotometer uses either a single or double beam [65]. Figure 5(a) shows the simplest single beam which is easy to utilize and compactible. It consists of the four basic components of absorption spectroscopy. A double beam, as shown in Figure 5(b), consists of two beams from the same source divided into two optical paths. The first beam passes through the reference and second beam passes through the sample. The main advantage of the double beam channel is the reference material makes the measurement more stable, precise and accurate compared to the single beam channel[60].

However, one of drawbacks of the double beam channel is the low of ratio signal-to-noise which affected the sensitivity of the system. In absorption spectroscopy, normally two types interference can occur namely spectra interference and interference from the absorption species[66]. Spectra interference appears from the overlapping line in monochromator. Interference filter are needed to limit the number of wavelength. Interference from the absorption species involves thick or opaque thin film. In thick thin film, the absorbance depends on the optical length path in the sample. To avoid this circumstance, diffuse reflectance measurement with integrated sphere can be used[67]. Derivative spectrophotometer is also one of the suitable methods for avoiding interference due to absorption species[68].

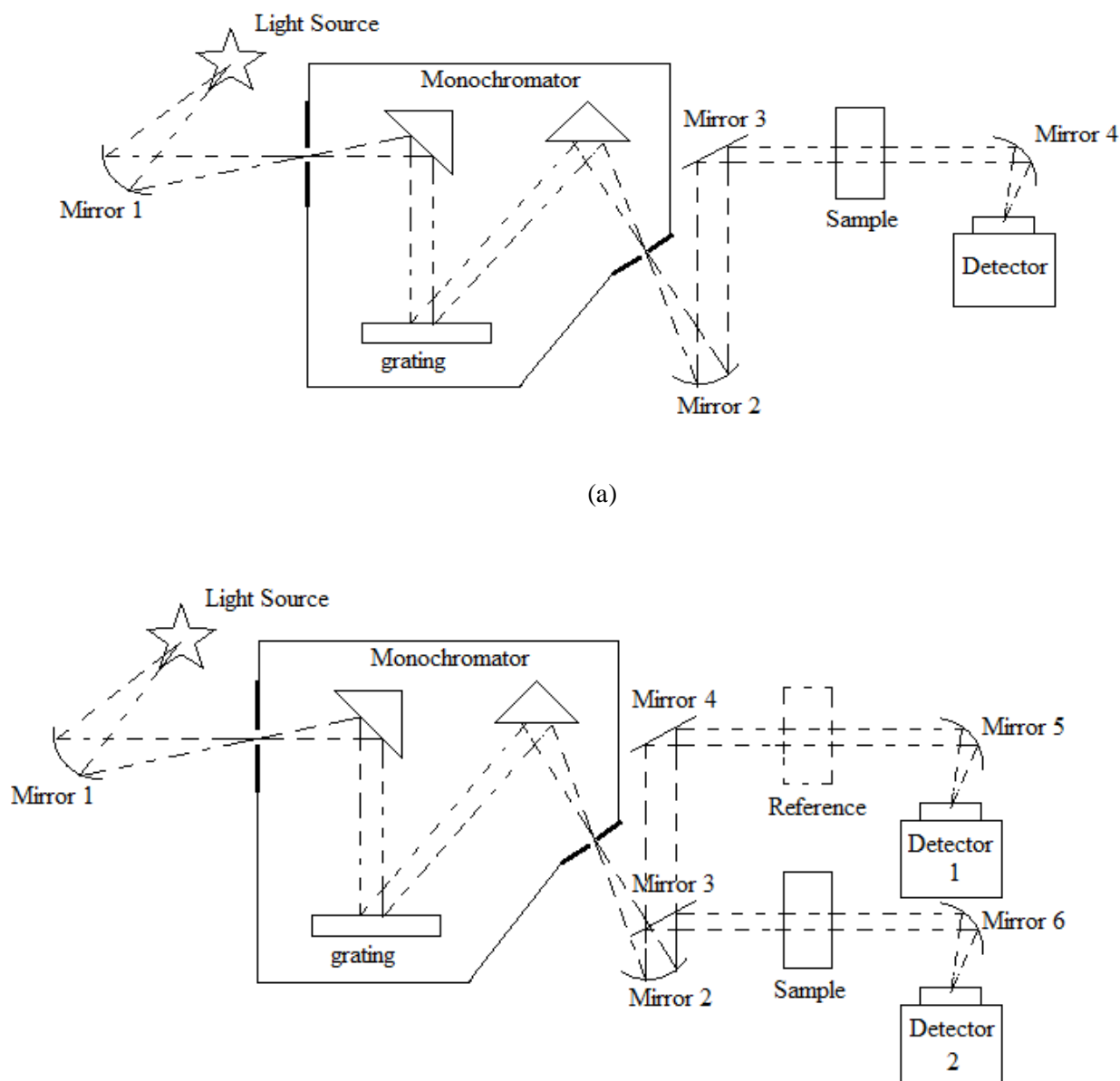


Figure 5: (a) Single- and (b) double-channel UV-vis spectrophotometers. Redrawn and adapted from reference [65].

In the absorption process, the intensity of light decreases when propagates in the medium as shown in Figure 6(a). The ratio intensity loss (dI/I) is proportional with small changes in the sample thickness dx . This relation can be given by equation (3).

$$\frac{dI}{I} = -\alpha dx \tag{3}$$

Lets I_0 is the initial or incident light intensity before entering the medium and x is the sample thickness. The intensity absorbed by the sample can be calculated by integration equation (3) of both side as;

$$\int_{I_0}^I \frac{dI}{I} = -\alpha \int_0^x dx$$

$$I = I_0 \exp(-\alpha x) \tag{4}$$

With i is the transmitted light and this equation is known as Lambert-Beer laws. According to this law, the light intensity exponentially decays with the sample thickness as shown in Figure 9(b). The coefficient of proportionality in equation (3) and (4) is known as absorbance coefficient and it measures how strong the sample absorbs light at a specific wavelength.

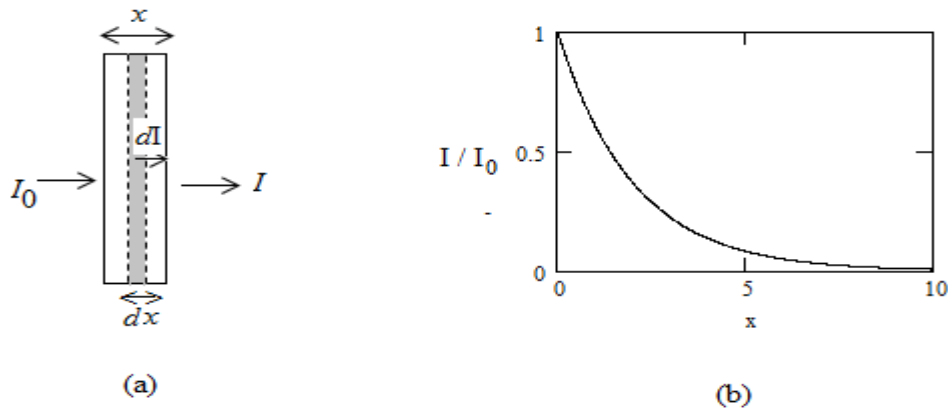


Figure 6 (a) The light absorption process in thin film (b) The normalized light intensity been absorb in the thin film as the function of sample thickness x with $\alpha = 0.5 \text{ m}^{-1}$

Ellipsometry and Optical Reflectometry

Optical reflectometry and ellipsometry are non-destructive and contactless tests based on the interaction between reflected light and a sample. The light reflected from a polymer surface characterizes the material properties of a polymer, such as the optical constant, surface roughness, and thickness. Optical reflectometry is simple and low cost because it uses non-polarized light as the optical source, such as a tungsten bulb. Ellipsometry is more complicated than optical reflectometry. Ellipsometry uses the effect of light polarization to characterize the optical properties of a material. Therefore, the instrument must be carefully setup to investigate the change in polarization state. The basic technical components of an ellipsometer are light source, polarizer, phase inducer, analyzer, and detector, as shown in Figure 7 (a)[69].

The light source for ellipsometry, which is commonly UV based, is deuterium light. Advance approaches use a single-wavelength laser. A laser is an optoelectronic device that electromagnetic waves by an optical amplification process through stimulated emission. The type of electromagnetic wave depends on the type of active material used to create an inverse population at the excited state. Angstrom Advance Inc. Use tunable lasers as the optical light source, and the wavelength can be selected [70]. A polarizer is an optical filter that changes the state of polarization of an electromagnetic wave. Light is polarized by changing the phase or direction of the vibrating amplitude.

Polarizer's come in many types, such as calcite, linear, wave plate, and wire grid polarizers [71]. Each polarizer converts the specific state of polarization to plane, elliptical, left, or right circular polarization. To achieve specific elliptical polarization, a phase inducer is used. A phase inducer can be a wave plate, compensator, or phase modulator [72]. The light reflected from the sample is analyzed by a polarized-type analyzer. Rotating analyzer ellipsometry using a compensator has been developed for real-time ellipsometry measurements [73].

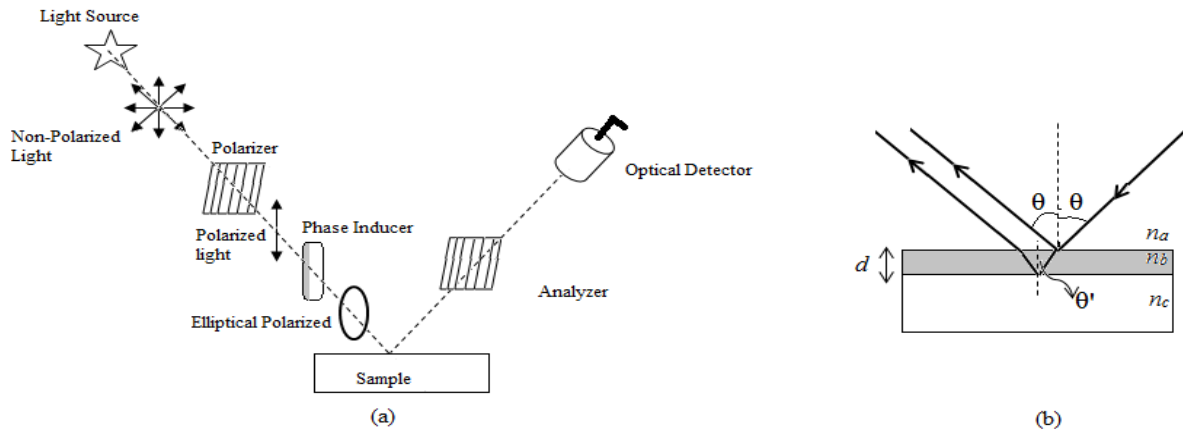


Figure 7(a) Ellipsometry schematic (b) Basic reflection in thin film. Redrawn and adapted from reference [69].

In the optical reflectometry and ellipsometry, the purpose of these measurements is to obtain the optical constant and film thickness. Reflection or reflectivity is commonly used to measure this parameter. Consider in the simple case, an incidence light propagates from ambient condition with refractive index n_a to a thin film with refractive index n_b as shown in Figure 10(b). According to Snell's law, the incident light will reflect in same medium and refract in the thin film. However, it may be again refracted at point Y. This optical beam splitting creates interference with the optical path difference, Δ equal to $2n_b d$. The total reflectance and thickness for this system is given by equation (5) and (6):

$$R = \frac{R_{ab}^2 \exp(\alpha d) + R_{bc}^2 \exp(-\alpha d) + 2R_{ab}R_{bc} \cos \varphi_1}{\exp(\alpha d) + R_{ab}^2 R_{bc}^2 \exp(-\alpha d) + 2R_{ab}R_{bc} \cos \varphi_1} \tag{5}$$

$$d = \frac{i\lambda_0 \lambda_i}{2n_b (\lambda_i - \lambda_0) \cos \theta'} \tag{6}$$

Where $R_{ab} = \frac{n_a - n_b}{n_a + n_b}$, $R_{bc} = \frac{n_b - n_c}{n_b + n_c}$, $\varphi_1 = \frac{4\pi n_b d \cos(\theta')}{\lambda}$, $\theta' = \sin^{-1} \left(\frac{n_a \sin \theta}{n_b} \right)$

And i is a constant which create adjacent fringe pattern to λ_0 to λ_i [69, 74].

Ellipsometry spectroscopy measures two parameters, namely, Ψ and Δ . Ψ is the angle tangent to the amplitude Fresnel coefficient upon reflection p (the polarized electrical field parallel to the plane) and s (the polarized electrical field perpendicular to the plane) polarization [75]. Δ is the phase shift when light experiences the reflection between p and s [76]. From the measured value of Ψ and Δ , we can characterize the physical properties of thin film such as surface roughness, band energy and optical dispersion behavior. The various characterizations using ellipsometry spectroscopy are shown in Figure 8. However, the spectroscopic ellipsometry has limitations such as involving reflection at small spot size and only applicable for high absorption coefficient [77]. Besides that, the optical modeling for data analysis in spectroscopic ellipsometry is quite complicated.

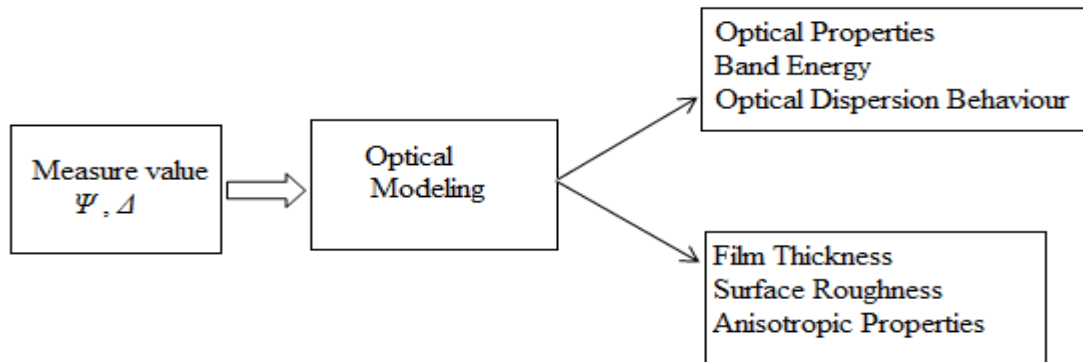


Figure 8: Characterization of physical properties by using Spectroscopy Ellipsometry.Redrawn and adapted from reference [77].

Flourescence Spectroscopy

Fluorescence or photoluminescence (PL) spectroscopy is an analytic tool for measuring the emission of light from a polymer molecule that is in an electronically excited state. Fluorescence spectroscopy is much more challenging than UV-vis absorption spectroscopy. In fluorescence spectroscopy, the main objective is to collect optical data from a sample after it is excited at a specific excitation wavelength. Fluorescence spectroscopy measurements can be performed by steady-state or time-resolved fluorescence spectroscopy.

As shown in Figure 9, two monochromators are used in fluorescence spectroscopy. The first is used to select the wavelength for excitation. The second is used to analyze the emitted wavelength from the sample. A photomultiplier is commonly used as a detector in fluorescence spectroscopy. An alternative to high-sensitivity detectors is a system that involves single photon counting [80]. Single photon counting allows a photodetector to detect single photons. This application is suitable for a sample that shows low emission intensity. According to the physics law of optic, the diffraction plays an important role in the fluorescence spectroscopy especially for detecting single molecule[81].

This is due to the diffraction limits are linearly proportional to the light wavelength[82]. By choosing suitable optical entrance slits and coupling lens, they can beat the diffraction limits in optical instruments system[83]. Optimizing setting in optical entrance slit and optical filter/bandpass are also important parameters to reduce second order diffraction effect which superimpose between emission spectrum and light scattered from holographic grating[84].

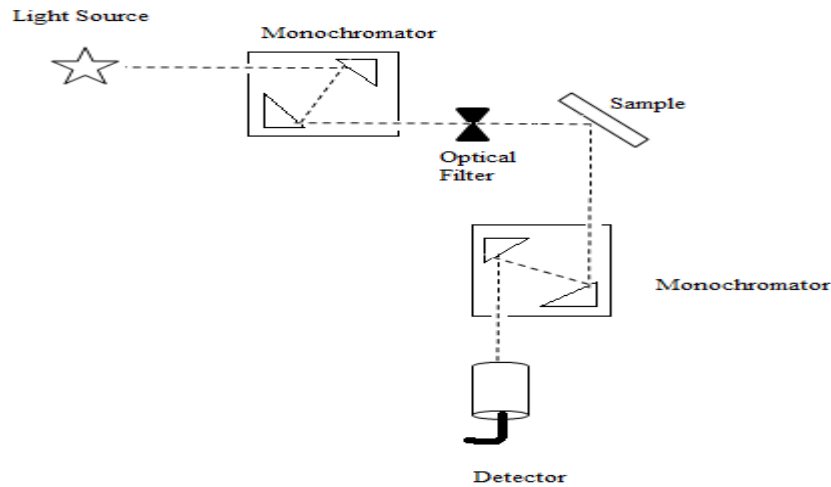


Figure 9: Schematic of fluorescence spectroscopy. Redrawn and adapted from reference [78].

The luminescence process in solid involves interaction electronic state of material with electromagnetic radiation. In early approach, classical theory has been used to explain this behavior but classical theory failed to explain a few phenomenon of luminescence. However, classical theory is capable to explain very board range in optical problem[85]. In the classical approach, excitation and emission process involving energy transfer between electromagnetic radiation and electric or magnetic dipoles, quadrupoles, octupoles, rotator and so on. This interaction can be described by using harmonic oscillator model. Electronic transition in atoms for normalized line width of spontaneous emission is given by [86]:

$$S(\nu_{lm}, \nu) = \frac{1}{2\pi^2} \left(\frac{\Delta\nu_N}{(\nu_{lm} - \nu)^2 + (\Delta\nu)^2} \right) \quad (7)$$

Where $\Delta\nu_N = 1/2\pi\tau_m$, τ_m is the life time of upper state, ν_{lm} is centered frequency and $\Delta\nu$ is the uncertainty of frequency. In quantum mechanics approach, basically the processes involve excitation, spontaneous emission and stimulated emission. Meanwhile, the excitation and emission processes involve quantized and discrete energy. Let E_1 and E_2 is the energy level for ground state and excitation state. The number of population of E_1 and E_2 are n_1 and n_2 respectively. This population can be represented by Boltzmann distribution;

$$\frac{n_2}{n_1} = \exp\left(-\frac{E_2 - E_1}{kt}\right) = \exp\left(-\frac{h\nu_{12}}{kt}\right) \quad (8)$$

Where ν_{12} is the transition frequency from E_1 to E_2 . In steady state condition, the absorption rate is equal to the total stimulated and spontaneous emission rate which can be written as

$$B_{12}n_1\rho(h\nu_{12}) = b_{21}n_2\rho(h\nu_{12}) + A_{21}n_2 \quad (9)$$

Where $\rho(h\nu_{12})$ is the photon field energy density, B_{12} , B_{21} and A_{21} are constant[87].

Raman Spectroscopy

Raman spectroscopy is a vibration spectroscopy to measure the light scattering in solid. These vibrational characteristic spectra can be a finger print for the identified material. Raman spectroscopy can be used for both quantitative and qualitative analysis. Raman spectroscopy has several advantages such as non-destructive test, little or no sample preparations are required, low vapor water and CO₂ scattering which no need special purging system[88]. The basic Raman system consists of four major components that are laser, sample illumination system, wavelength and detector. Raman spectra are required coherent light source such as laser of ultraviolet (uv), visible (vis) or near infrared range. Laser produces a beam of light through a combination of stimulated emission, resonance cavity and optical pumping mechanism. Argon ion, krypton, helium-neon, Nd-YAG and laser diode are normally used as light source in Raman spectroscopy.

However, the main challenge in Raman spectroscopy is the efficiency of Raman scattering and competition with fluorescence spectra[66, 89]. For this reason, a specific sample illumination system is needed. In this paper, we only discuss a few illumination systems. In conventional sampling system (Figure 10), the technique is similar with the fluorescence and uv-vis absorption spectroscopy as discussed in section 3.1 and 3.4.

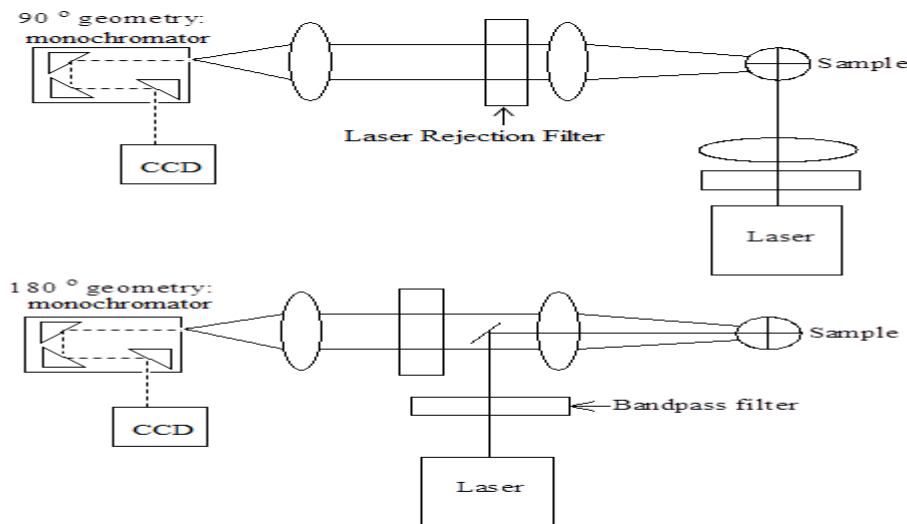


Figure 10: (a) Conventional sampling with 90° (upper) and 180° (lower) optical geometry Redrawn and adapted from reference[89]

The intensity of the Raman scattering are very weak compared to the Rayleigh scattering. Rayleigh scattering is also known as elastic scattering. In the Rayleigh scattering, the particle is assumed smaller than that of light wavelength. In this case, the incident photon energy is conserved. Meanwhile, inelastic scattering is a scattering process where the kinetic energy is not conserved. The incident photon energy is absorbed or emitted by photon. Brillouin scattering is a process where phonon absorbed or emitted in an acoustic mode. Raman scattering also involves in optical mode. From the conservation of energy and momentum, the absorbed phonon is known as anti-Stokes component.

Whilst for Stokes component, it involves emitted of phonon. Both components are shown in Figure 11.

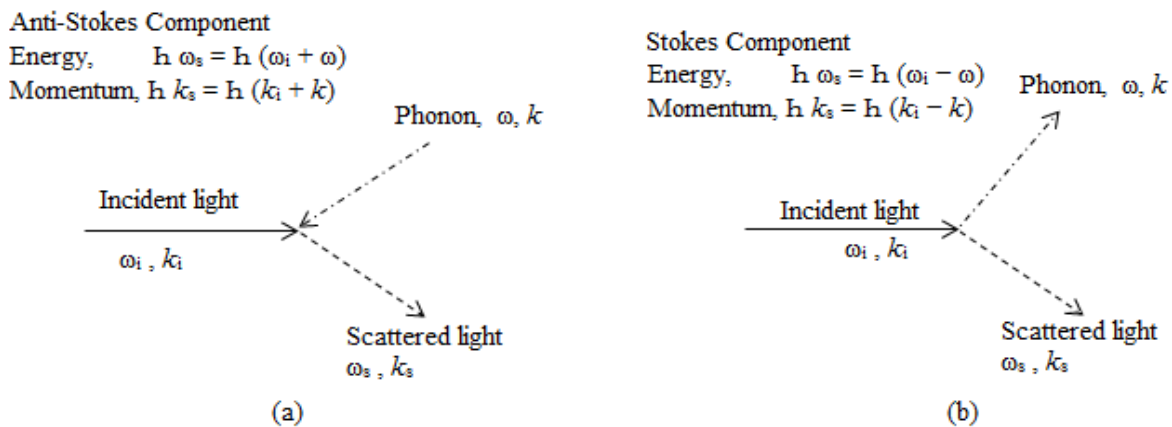


Figure 11 (a) anti-Stokes component and (b) Stokes component. The symbols of ω and k represent frequency and momentum. Subscript i and s represents incident light and scattered light, respectively.

Since the signals obtained from Raman scattering are weak. Therefore, a few approach has been used to enhance the signals such as Resonance Raman Scattering (RRS), stimulated Raman scattering, surface enhance Raman scattering (SERS) and coherent anti-stokes Raman scattering. In this paper, we only discuss Resonance Raman Scattering (RRS) in which the application can be used to investigate the conjugation length in polymeric system. In RRS, excitation laser beam and tunable laser chosen is comparable with the electronic transition and excitation light source, respectively.

The frequency has the energy different between ground vibration state and the first or second vibration state of excitation state. It is noted that the scattering process is much faster compared to the absorption process. In this case, scattering process can be distinguished from absorption process at particular time. When the incident frequency match with the electronic transition, then radiation from the molecule will enhance the Raman signal[90].

Interpretation of Optical Characterization Results

In order to understand the optoelectronic and photonic device behavior as mentioned in section 2, therefore it is better to first understand the optical properties of polymeric material. The optical properties of polymeric material implies the electronic structure which affect the electrical and optical output in properties of optoelectronic and photonic.

Optical Absorption Band and Localized State

The simplest method to investigate the electronic structure of a solid material is by studying its optical absorption. Absorption occurs when a photon has sufficient energy to excite electrons from the lowest energy to the highest energy. The fundamental equation between the absorption and energy gap E_g is given by $E_g = \hbar\omega$, where ω is the light frequency and \hbar is the Planck constant. Fundamental absorption refers to a band-to-band transition in the solid phase. In crystalline materials, direct transition occurs when electrons are excited from the valence band to the conduction band in the same k -space. In this process, the total energy and momentum is conserved. For indirect transition, electrons cross the conduction band at different k -spaces.

In this case, transition is possible only when phonon assisted. Given that the potential well fluctuates in amorphous materials, there is no specific definition in k -space (non-conservation of k -space) and electron localization (also known as Anderson localization) occurs[91]. According to the Davis–Mott model, the wave function is localized and the probability of transition depends on wave function overlapping [92]. Considering that amorphous materials lack a long-range order, a localized state extends from the conduction and valence bands to the band gap. This localized state can affect the electron transition in amorphous and polymeric materials.

The absorption coefficient α is related to the absorbance A based on the Lambert-Beer law in section 3.1 that is;

$$\therefore \alpha = 2.303A / x \quad (10)$$

Where x is the sample thickness. The optical absorption for non-crystalline materials is given by the Tauc and Davis–Mott model [93, 94]

$$(\alpha\hbar\omega)^n = \beta(\hbar\omega - E_{opt}) \quad (11)$$

Where β is a constant and n is the exponential constant index. The exponential constant index is an important parameter that describes the type of electronic transition. There are four types of transition in amorphous materials that can be represented with n . The values of n are commonly 1/3, 1/2, 2/3, and 2 for indirect forbidden, indirect allowed, direct forbidden, and direct allowed transitions, respectively[95]. A typical absorption plot for amorphous materials is shown in Figure 12. The optical absorption can be divided to three regions, namely, high-level absorption (A), exponential region (B), and weak absorption (C). High-level absorption is basic optical transition. Whereas the weak absorption region is below the exponential region which depend on the sample preparation, impurity, and thermal annealing history [96].

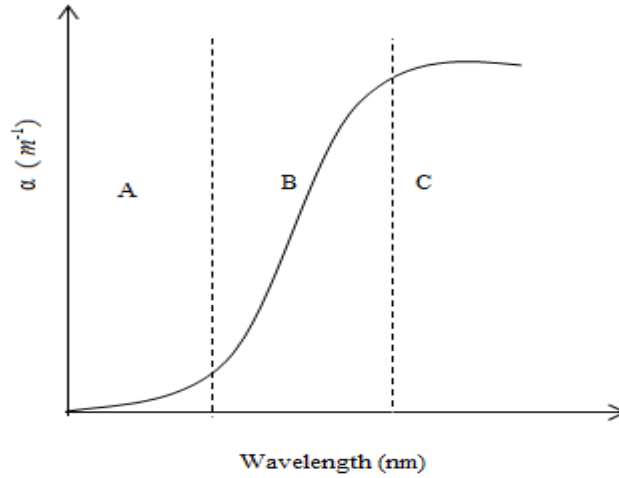


Figure12: Typical absorption spectra for amorphous materials.

The exponential region was first observed by Urbach in an absorption experiment [97]. This region is called the Urbach edge, which depends on the photon energy. Dexter expressed the empirical relation of the Urbach edge as

$$\alpha(\hbar\omega) = \alpha_0(T) \exp(\sigma(\hbar\omega - E_0)/kT) \quad (12)$$

Where α_0 is the normalized transition strength as a function of the absolute temperature, and σ and E_0 are constants [98]. This expression is based on the existence of an internal electrical field inside a material. Redfield further found that the existence of an internal electrical field is due to the charge defect in solids [99]. Dow pointed out that an electrical field induces the ionization of excitons [100]. Toyozawa proposed that interactions between excitons and electron lattices create the Urbach region [101]. However, Skettrup argued the effects of electron-lattice interactions [102] and suggested that thermal fluctuations in energy gaps create the absorption tail.

All the above models are applicable for polymeric materials. The electronic structures of polymers are highly complicated. Bond orders and polymer backbone kinks also affect the electronic structure of polymers. According to the Franck-Condon rule, the fluctuation of the lattice configuration in polymers smears the fundamental edge and produces the Urbach tail [103]. Kinks in polymer backbones create a localization state at the gap center, known as a soliton. The existence of a soliton can change physical and optical absorption properties. However, solitons can be successfully described in polyacetylene. Most conducting polymers such as PPV, PPP, polythiophene, polyaniline, and poly(N-carbazole) (PVK) contain defects because order parameters create quasi-particle charges that are soliton-antisoliton pairs, polarons, or bipolarons [104].

These quasi-particle entities produce discrete energy levels in the bandgap and reflect the absorption coefficient. Electronic states play an important role in the fundamental absorption edge. From Eq. (7), we can plot α vs. Energy ($\hbar\omega$), $(\alpha\hbar\omega)^{1/2}$ vs. $\hbar\omega$, or $(\alpha\hbar\omega)^2$ vs. $\hbar\omega$ to obtain the fundamental absorption edge E_u , direct allowed optical transition e_d , and indirect allowed optical transition E_i by extrapolation to the $\hbar\omega$ axis. Figure 13 illustrates the different plots of α for PVK. From this figure, the value of E_u , E_d and e_i for PVK is 4.04, 4.23 and 3.75 eV respectively with thickness of 150 nm. For the Urbach edge E_e , we can calculate the extended state by plotting $\ln\alpha$ vs. $\hbar\omega$. The values of E_u , e_d , E_i , and E_e strongly depend on the thin film thickness [105, 106].

Table 1 shows the optical absorption parameter of MEH-PPV, PVK, polythiophene, polyvinyl alcohol (PVA), and poly(N-benzyl aniline) (pbani). Most of these polymers have been blended with different polymer materials or composites and inorganic materials to enhance the optical properties of polymer systems. As aforementioned, the optical properties of polymers strongly depend on the preparation conditions, as shown in Table 1. Different preparation methods of MEH-PPV yield different values of E_d [62, 64, 107]. In addition, the thermal history also plays important roles in optical properties. Although pbani does not contain any impurity, the annealing temperature changes the Urbach edge and E_d [108].

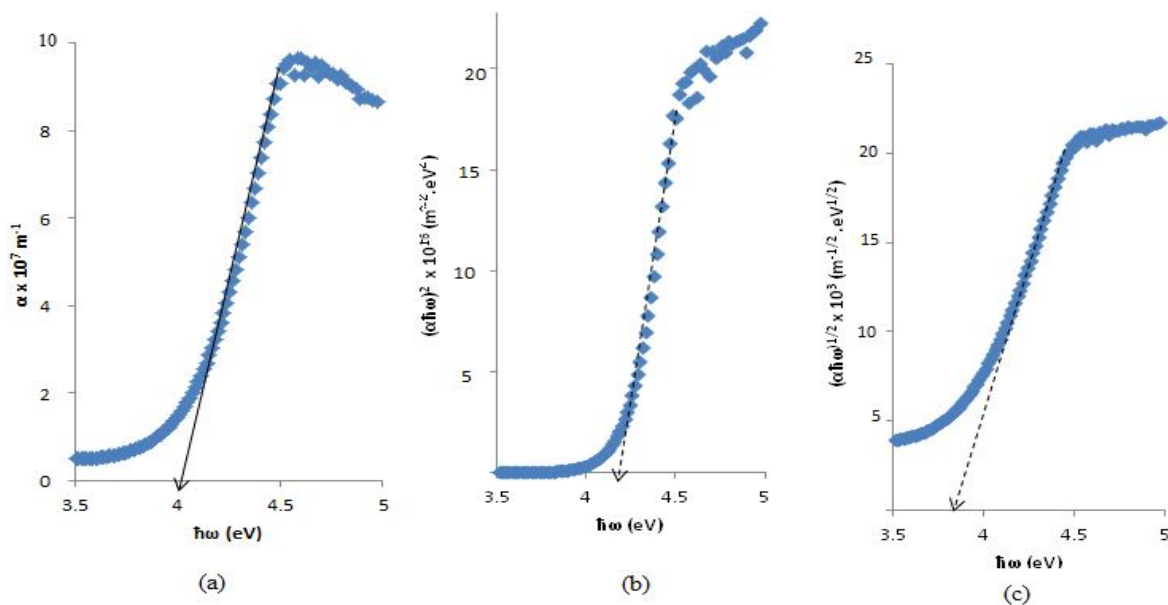


Figure 13 Plot (a) α vs. Energy ($\hbar\omega$), (b) $(\alpha\hbar\omega)^{1/2}$ vs. $\hbar\omega$, and (c) $(\alpha\hbar\omega)^2$ vs. $\hbar\omega$ for PVK. Reprinted from Advanced Materials Research Vols. 488-489, A. N. Alias, Z. M. Zabidi, T. I. T. Kudin, M. K. Harun, M. Z. Yahya, *Optical Characterization of Luminescence Polymer Blends Using Tauc/Davis-Mott Model*, Pages 628-632, Copyright (2012), with permission from Scientific.net.

Table 1 Values of thickness, absorption edge (E_c), allowed direct bandgap(E_d), allowed indirect bandgap(E_i), and Urbach edge (E_u)

Host polymer	Impurities	Thickness (nm)	E_c (ev)	E_d (ev)	E_i (ev)	E_u (ev)	Ref.
MEH-PPV	–	100		2.180			[62]
	–	–		2.070			[64]
	Blending with mesocarbonmicrobead 5%	–		2.100			[64]
	–	34.50		2.194			[107, 109]
	5 wt% zno	40.51		2.166			[107, 109]
	10 wt% zno	44.51		2.130			[107, 109]
	15 wt% zno	4.35		2.122			[107, 109]
	20 wt% zno	51.36		2.134			[107, 109]
Poly(N-carbazole)	–	150	4.040	4.230	3.75	0.258	[110]
	50wt% PVDF-hfp	154	4.050	4.220	3.830	0.244	[110]
	10wt% PVP	360.3	3.380	3.433	3.208	0.111	[111]
	20wt% PVP	495.1	3.417	3.453	3.225	0.208	[111]
	30wt% PVP	388.0	3.438	3.497	3.300	0.189	[111]
	40wt% PVP	384.5	3.457	3.501	3.363	0.128	[111]
	50wt% PVP	420.0	3.470	3.512	3.399	0.139	[111]
	60wt% PVP	372.6	3.475	3.519	3.410	0.227	[111]
PEDOT:PSS	10wt% PANI			3.880	3.430	0.390	[112]
	20wt% PANI			3.860	3.431	0.440	[112]
	50wt% PANI			3.830	3.23	0.530	[112]

PVA(before annealing)	–	Range, $1.9-3 \times 10^{-7}$		6.272	5.902	0.742	[113]
	5% niCl ₂	Range, $1.9-3 \times 10^{-7}$		5.576	5.193	0.236	[113]
	10% niCl ₂	Range, $1.9-3 \times 10^{-7}$		5.484	5.117	0.201	[113]
	15% niCl ₂	Range, $1.9-3 \times 10^{-7}$		5.384	5.067	0.189	[113]
PVA (after annealing at 70 °C)	–	Range, $1.9-3 \times 10^{-7}$		6.251	5.889	0.753	[113]
	5% niCl ₂	Range, $1.9-3 \times 10^{-7}$		5.479	5.102	0.258	[113]
	10% niCl ₂	Range, $1.9-3 \times 10^{-7}$		5.381	5.026	0.220	[113]
	15% niCl ₂	Range, $1.9-3 \times 10^{-7}$		5.282	4.934	0.214	[113]
Pbani (different annealing temperatures)							
25 °C	–	110		2.090		0.540	[108]
55 °C	–	110		2.080		0.55	[108]
115 °C	–	110		2.070		0.58	[108]
145 °C	–	110		2.050		0.60	[108]

Refractive Index and Dispersion Behavior

The interactions between electromagnetic waves and polymers elucidate the condensation properties of polymers, including their electronic state, vibration state, and binding energy. In the visible region, based on Snell's law, when light propagates in a material, the velocity of a material is distorted. This ratio changes with the light velocity and yield the optical constant as the refractive index. This refractive index is a fingerprint of a polymeric material. When light propagates in the polymer at one velocity in all directions, the polymer is called an isotropic polymeric material. When light propagates in the polymer at different velocities in only one direction, the polymer is called an anisotropic polymeric material. Considering the complexity of the condensation properties of a polymeric system, the refractive dispersion behavior and optical dielectric spectra of polymeric systems must be understood to apply them in optoelectronic and photonic devices.

The optical dispersion of a polymer can be determined by transmission measurements or interferometry [114, 115]. Each measurement is used to obtain a complex optical dielectric constant and refractive index given by Eqs. (13) and (14).

$$N = n_r + i n_i \quad (13)$$

$$E = \varepsilon_r + i \varepsilon_i \quad (14)$$

The complex dielectric constant is a fundamental intrinsic property of a material. The real part of the dielectric constant shows how much it can slow down the speed of light in a polymeric material. The imaginary part shows how a dielectric in the polymer absorbs energy from an electric field caused by dipole motion[116]. The real and imaginary parts of the dielectric constant are related to the refractive index by Eqs. (15a) and (15b).

$$E_r = n^2 - k^2 \quad (15a)$$

$$E_i = 2nk \quad (15b)$$

Where k is the extinction coefficient and given by $k = \alpha\lambda/4\pi$. From Maxwell's equation, the refractive index is given by Eq.(16).

$$N^2 = \varepsilon = 1 + P = 1 + 4\pi (\chi_e + \chi_l) \quad (16)$$

Where β is the polarization, χ_e is the electronic susceptibility, and χ_l is the lattice susceptibility. We can fit the equation using the harmonic oscillator shown in Eq.(17)

$$n^2 = 1 + \frac{a_1 \lambda^2}{\lambda^2 - \lambda_1^2} + \frac{a_2 \lambda^2}{\lambda^2 - \lambda_2^2} + \frac{a_3 \lambda^2}{\lambda^2 - \lambda_3^2} + \dots = 1 + \sum_{j=1}^m \frac{a_j \lambda^2}{\lambda^2 - \lambda_j^2} \dots \dots \dots (17)$$

Eq.(12) is also known as the Sellmeier equation; a_j and λ_j are the sellmeier coefficients. Moss simplified the Sellmeier equation into eq.(18) [117]

$$n^2 - 1 = \frac{S_0^2 \lambda_0^2}{(1 - \lambda_0^2) / \lambda} \tag{18}$$

Where the average Sellmeier oscillator strength S_0 is related to $S_0 / \lambda_0 = n_\infty^2 - 1$, n_∞ is the infinite or high-frequency refractive index, and λ_0 is the average oscillator wavelength. The real and imaginary parts of optical dispersion are obtained from the Kramers–Kronig relation, and sums up the rules for the linear optical function. The Kramer–Kronig relation for complex real and imaginary dielectric constants is given by Eq.(19)

$$\varepsilon'(\omega) = 1 + \frac{2}{\pi} P \int_0^\infty \frac{\omega' \varepsilon''(\omega')}{\omega'^2 - \omega^2} d\omega' \tag{19a}$$

And

$$\varepsilon''(\omega) = 1 + \frac{2\omega}{\pi} P \int_0^\infty \frac{\varepsilon'(\omega')}{\omega'^2 - \omega^2} d\omega' \tag{19b}$$

Where ω' is the integration variable and P is the principle values of integrals. In solving the Kramer–Kronig relation, numerous approaches can be used to fit with the experimental result. The equation commonly used are the Adachi model[118], Penn model[119], Forouhi–Bloomer relation[120, 121], Philips model [122], and Moss relation[123]. The single effective oscillator model is the refractive index dispersion model that fits with the experimental result to determine the single oscillator energy E_0 and dispersion energy E_d [124]. Based on this model, the refractive index dispersion is given by

$$n^2 - 1 = \frac{E_d E_0}{E_0^2 - (\hbar\omega)} \tag{20}$$

By plotting $(n^2 - 1)^{-1}$ vs. $(\hbar\omega)^2$ a straight line is obtained. E_0 and E_d are then determined from the slope and intercept on the $(\hbar\omega)^2$ axis. The interband transition strength moment M_{-1} and M_{-3} can be calculated from the single-effective oscillator energy and dispersion energy using Eq. (21) [125]. The values of E_0 , E_d , as well as interband transition strength moments m_{-1} and M_{-3} of the current blending polymer system are shown in Table 2.

$$E_d^2 = \frac{M_{-1}^3}{M_{-3}} \quad E_0^2 = \frac{M_{-1}}{M_{-3}} \tag{21}$$

Table 2: Values of the Sellmeier and Wemple–didomenico optical parameters

Host polymer	Impurities	N_{∞}	A_0	$S_0, \times 10^{13}$ (m^{-2})	E_d (ev)	E_0 (ev)	Ref.
MEH-PPV	10wt% C ₇₀	1.93	319.28	2.68	10.61	3.89	[126]
PVK	10wt% PVP	1.907	233.910	4.819	13.800	5.050	[127]
	20wt% PVP	2.032	246.786	5.138	15.302	5.095	[127]
	30wt% PVP	2.150	247.435	5.917	18.558	5.148	[127]
	40wt% PVP	2.273	244.122	6.991	29.758	5.244	[127]
	50wt% PVP	2.610	240.084	10.083	30.359	5.278	[127]
	60wt% PVP	2.118	242.466	5.929	17.900	5.195	[127]
PEDOT:PSS	9:1 PEDOT:PSS/zno				100.00	4.00	[116]
	8:2 PEDOT:PSS/zno				80.00	4.00	[116]
	7:3 PEDOT:PSS/zno				65.59	4.07	[116]
	6:4 PEDOT:PSS/zno				59.31	4.15	[116]
PVA	–	1.394	217	1.590	4.96	8.150	[128]
	5wt% cecl ₃	1.426	222	1.77	5.1	7.21	[128]
	7wt% cecl ₃	1.496	231	2.22	6.59	7.01	[128]
	10wt% cecl ₃	1.515	250	2.38	6.98	6.81	[128]
	15wt% cecl ₃	1.557	252	2.65	7.12	6.21	[128]
Pbani (different annealing temperatures)							
	25 °C	6.37		1.15			[108]
	55 °C	5.71		1.03			[108]
	115 °C	5.76		1.05			[108]
	145 °C	5.96		1.11			[108]

Anisotropic Optical Spectra

Anisotropic optical measurements are based on the interaction between polarized electromagnetic waves and a polymeric material. The anisotropic optical spectra can be experimentally analyzed either by absorption- or reflectance-based anisotropic approaches. The absorption based anisotropy and the reflectance based anisotropy can be performed using linear polarized absorption spectroscopy and ellipsometry spectroscopy, respectively. In order to get linear polarized light, linear polarizer can be added in uv-vis absorption spectroscopy as mentioned in section 3 before being passing through the sample. Light polarization can be used to determine the direction or orientation of light within a molecule, which is important in investigating the effect of disorders in impurity systems such as polymer composites, dyes, and polymer blends.

The theoretical framework of the orientation of the host polymer with respect to the guest or dye molecule is found in literature [129]. When a material absorbs light, the molecules become excited and move to a higher energy level. The intensity of light absorption is proportional to the transition moment vector M as well as to the angle between M and the electrical field of light source [130]. M is the transition moment between the initial and excited states. This moment vector is related to the molecular symmetry and electric dipole moment operator [131]. The polarization ρ is an important parameter consisting of the observed perpendicular (I_{\perp}) and parallel (I_{\parallel}) polarized absorption intensity, as represented by Eq. (21) [132].

If the absorption is ideal and completely polarized in parallel direction, ρ is equal to +1 and vice versa for ideal polarized in perpendicular direction which ρ is equal to -1 [133]. Therefore, the polarization parameter range is -1

$$\rho = \frac{I_{\parallel} - I_{\perp}}{I_{\parallel} + I_{\perp}} \quad (22)$$

Most fabrication processes of polymer-based optoelectronic and photonic devices use spin coating or self-organization onto the substrate, and considers the morphology particularly the stiffness of the polymer backbone. All anisotropic geometries (e.g., disk- or rod-like) can influence the emission properties of LEDs [134]. Therefore, another approach that is ellipsometry spectroscopy can be used to determine the structure, morphology, and arrangement of molecules in polymer films. Ellipsometry spectroscopy measures two parameters, namely, Ψ and Δ which already discuss in section 3.2. Figure 14 shows the Ψ and Δ values of MEH-PPV with different thicknesses obtained from Gaudinet et al. [135].

They found that the changes in ellipsometry parameters are due to reflectivity and interference effects at the polymer material interface. The anisotropic optical property of MEH-PPV also depends on its molecular weight. High-molecular-weight MEH-PPV has a chain segmental orientation parallel to the layer plane, whereas low-molecular-weight MEH-PPV has a randomly oriented chain segment [136]. Tammer and Monkman reported that MEH-PPV has a rigid rod-like structure that forces it to be aligned parallel to the surface plane [137]. A similar observation was reported by Y.W. Jung et al., which implies that the MEH-PPV backbone lies in the plane of the film [138].

The polymer/contact interface is a significant factor affecting the performance of polymer-based electronic devices. The orientation of a polymer causes the dipole moment to align near the polymer/contact interface [139], resulting in the confinement of carriers near the interface [140]. The in situ electro-anisotropy reflection technique can be used to study the effect of the orientation and space charge at the polymer contact [141]. Schubert et al. found significant changes in ellipsometry parameters using different n- and p-type silicon substrates [142]. The changes are due to the existence of polariton propagation near the interface. A similar observation was reported by Mauger and Moule, who found that the changes in the anisotropic optical parameters at the interface of PEDOT:PSS are due to the lack of charge carrier absorption in the infrared region [143].

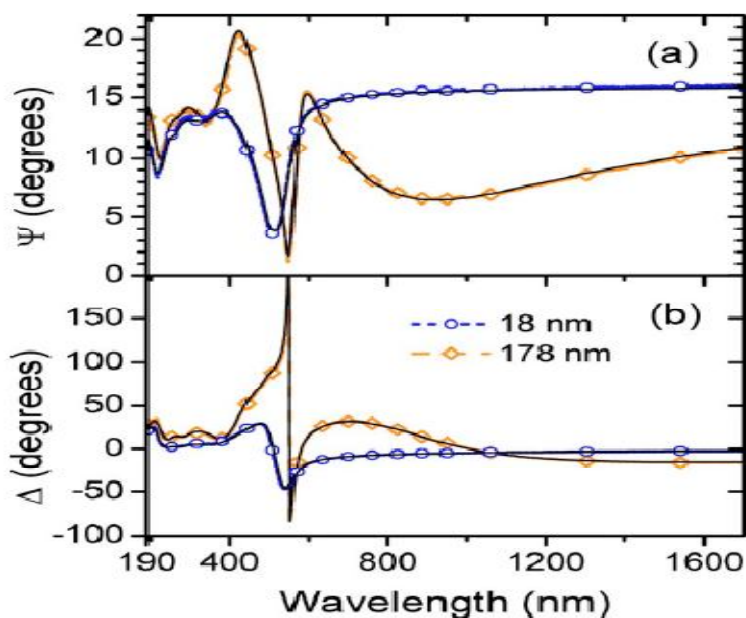


Figure 14: Simulated and experimental studies on MEH-PPV at different thicknesses. Reprinted with permission from Gaudin, O.P.M., et al., *Thickness dependent absorption spectra in conjugated polymers: Morphology or interference?* Applied Physics Letters, 2010. **96**(5): p. 053305. Copyright 2010, American Institute of Physics.

Emission and Excitation Spectra

In fluorescence and PL spectroscopy, fundamental measurements are based on excitation and emission spectra. Sole et al. well defined the differences between excitation and emission spectra, and further gave good examples [144]. Excitation spectra represent the absorption processes at a fixed emission wavelength. Emission spectra represent the emission process at a fixed excitation wavelength. The Jablonski energy level diagram shown in Figure 15 is commonly used to understand the photophysical and photochemical processes of the excited state. The ground, first-excited, and second-excited states are denoted as S_0 , S_1 , and S_2 , respectively.

S denotes a single state and t_1 denotes a triplet excited state. Each electronic state has discrete vibrational and rotational energies. Vibrational relaxation is a decay process that occurs after the electrons of a molecule move from a high vibrational energy level to the lowest vibrational energy level at the same electronic state. The lifetime of vibration relaxation is about (10^{-14} s to 10^{-12} s) [145]. Internal conversion is the non-radiative emission process from a high singlet excited state to a low excited state. From the lowest vibration state S_1 , an excited molecule can convert to the triplet state with a change in spin.

This process is called intersystem crossing. There are two types of radiative transition, namely, fluorescence or phosphorescence. Fluorescence is the radiative transition from the lowest excited state to the ground state with a short lifetime. Phosphorescence is the radiative transition from the lowest triplet state to the ground state with a longer life time (10^{-5} min to several minutes)[145].

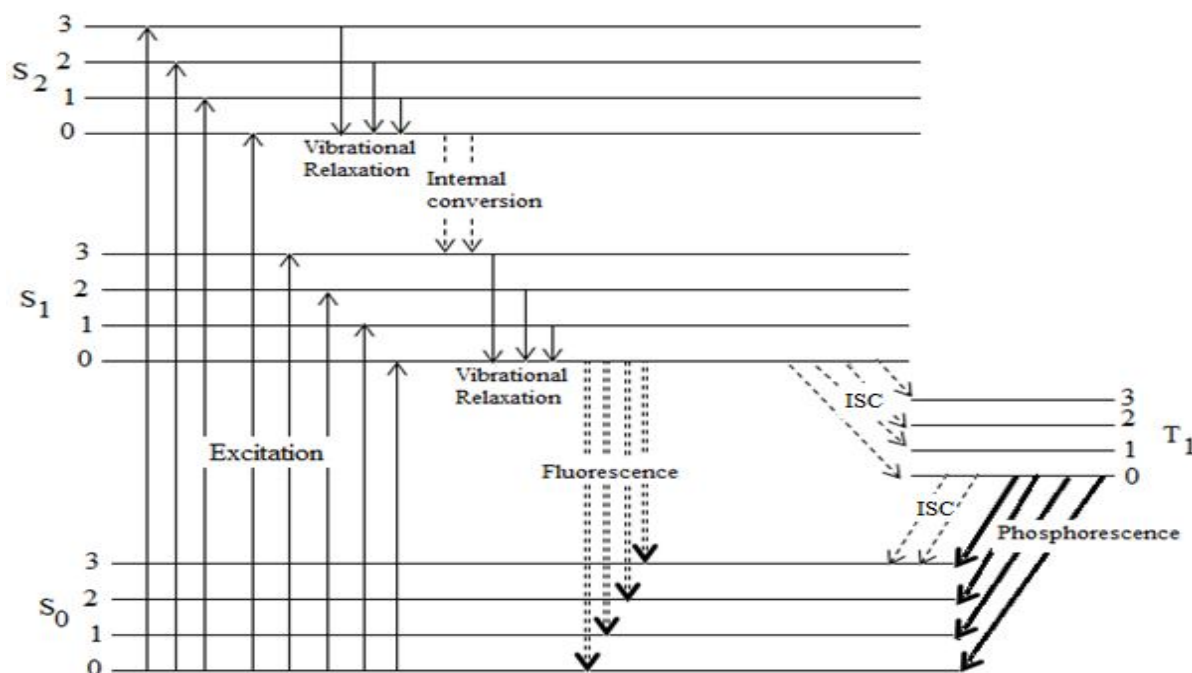


Figure 15: Jablonski diagram for the photophysical processes of fluorescence and phosphorescence. Isc mean intercrossing system. Redrawn and adapted from reference[130].

The theoretical modeling of the luminescence process is highly complicated because in polymeric and small-molecule materials, not all molecules are involved in luminescence. Only certain molecules that are electronically localized are involved. The same is true for solid-state physics wherein the process of luminescence occurs at the luminescence center [146, 147]. Another way to explain the luminescence mechanism is by the configuration coordinate diagram. Figure 16 shows the typical configuration coordinate diagram for the excitation and emission processes, with emphasis on the atomic rearrangement[148]. The assumptions that must be made when using the configuration coordinate diagram are as follows:

(1) the curve must be parabolic, and (2) the transition represented by a straight line and the system act as a harmonic oscillator[149]. According to Stoke's law, the emission energy must be less than or equal to the excitation energy. The difference between the excitation and emission energies is designated as W . The excitation spectrum is energy dependent, and pl consists of two parts, namely, light absorption by defects created in the localized state and by absorption in the Urbach edge[150]. If the excitation energy is less than the emission energy, the process is called anti-Stoke's law and the material is called up-conversion material.

By blending with other polymers or hybrid polymer-inorganic semiconductors, disorders are created in a thin film solid system. According to Sprenger, there are four basic transitions in a disorder system that affects the luminescence and dielectric properties: peak-to-peak, tail-to-tail, tail-to-peak, and peak to tail transitions [151]. These transitions can be observed as a shift in the maximum emission or excitation wavelengths and a decrease or increase in the emission or excitation intensity.

The shifts in excitation and emission spectra in the PVK blend with PVP at different composition ratios have been observed by Alias et al.[110]. They suggested that shifts in luminescence spectra are due to the aggregation of luminescence chromophores originating from complex physical bonding in a polymeric system. The photophysical properties of conjugated polymers strongly depend on the preparation conditions, such as the type of solvent used for purification and annealing treatment[152]. Consequently, the conjugation length is changed and the optical and electrical properties of the polymer are affected.

In a hybrid-conjugated polymer system, nanoparticles such as TiO_2 , ZnO , CdS , and CdSe have been used to optimize the device performance. Nanoparticles act as sensitizers or emitters upon light absorption. Nanoparticle addition leads to different luminescence spectrum properties. Figure 17 shows the PL spectra of pure MEH-PPV and MEH-PPV/ ZnO with different weight fractions. The changes in luminescence spectra are due to shallow or deep defect level states induced by nanoparticles [153]. This defect level leads to the localization of electrons, and hence, shifts in the luminescence spectra of a hybrid-polymer system[154].

The cluster shapes and sizes of nanoparticles in a hybrid-polymer system influence the luminescence spectra. Petrella et al. showed that nanocrystal TiO_2 with a rod-like shape shows higher luminescence quenching than dot-shaped ones [155]. Therefore, the configuration coordination diagram shows that when a polymeric system absorbs energy and creates an excited state, the changes in Δr depend on the size and molecular weight of the host polymer, as well as on the size and charge localization of the sensitized cell.

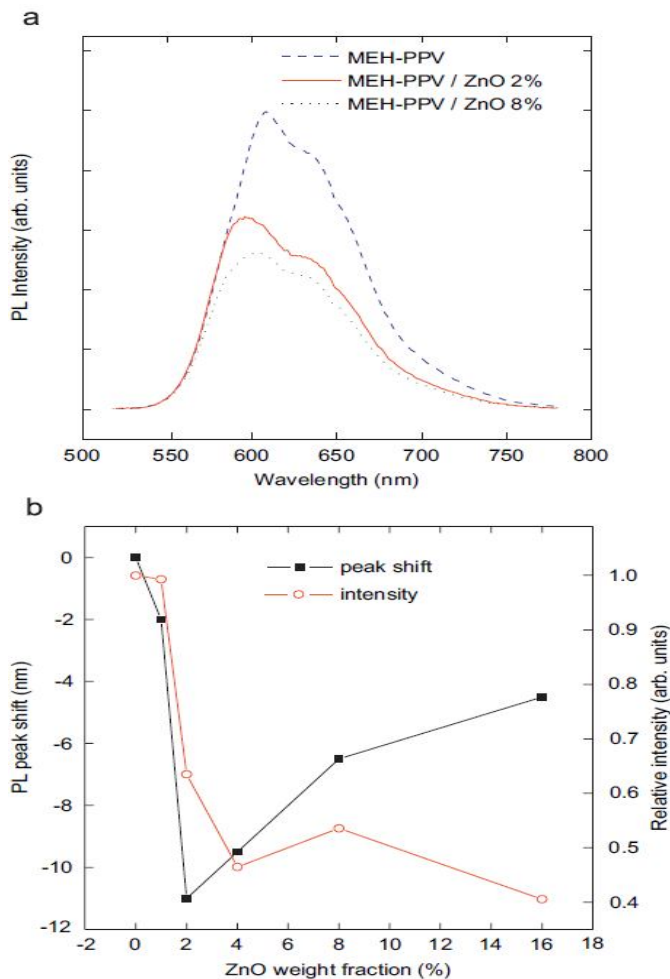


Figure 17: (a) PL spectra of pure MEH-PPV and MEH-PPV/ ZnO with percentage weight fractions of 2% and 8%. (b) variations in PL peak shifting and intensity of MEH-PPV/ ZnO at different weight fractions[153]. Reprinted from journal of Luminescence, Vol128, Ton-That, C., M.R. Phillips, and T.-P. Nguyen, *Blue Shift in the Luminescence Spectra of MEH-PPV Films Containing ZnO Nanoparticle*, Pages 2031-2034, Copyright (2008), with permission from Elsevier.

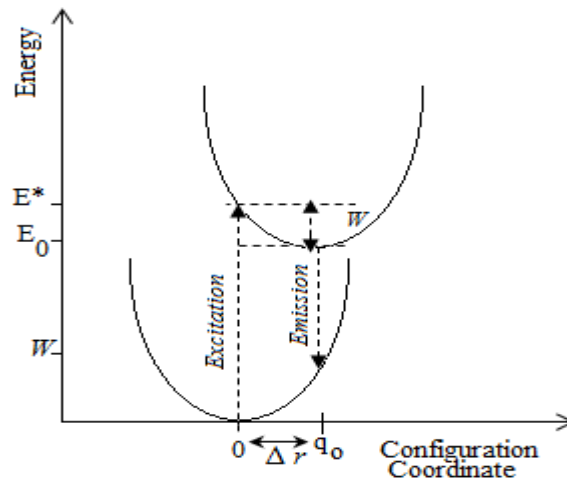


Figure 16: Typical configuration coordinate diagram. Redrawn and adapted from reference [148].

Raman Spectra

In section 4.1 and 4.4, we already mentioned that the impurities could affect the absorption, excitation and emission spectra. One of the reason for the changes in these spectra are due to the changes in extended π -electron system which affected delocalization length or conjugation length[156, 157]. It is well known that Raman analysis can be used to analysis the conjugated segment in polymer. Conjugation length can lead to the increasing or decreasing of frequency as well as Raman intensity which corresponding to vibration mode in conjugation. Complete analysis vibration mode of Raman intensity for poly(p-phenylenevinylene) [158] , C60[159], carbazole[160], polythiophene[161], polyfluorene[162] and *trans* and *cis*polyacetylene[163, 164]are reported.

Raman intensity and frequency in conjugated polymer also strongly depend on the intra-chain order formation [165]. Furthermore, the different of structural phases in crystalline and glass state change the frequency dispersion which could be connected with the changes in the conjugation length[166]. In theoretical modeling, Resonance Raman scattering (RRS) in cross sectional of PPV $\alpha_f(\Omega_L, \omega)$ for each vibrational mode f is given by equation[167];

$$\alpha_f(\Omega_L, \omega) \approx \sum_{n=2}^{10} |M_n|^4 S_{f,n} \times \left| \sum_{l=0}^1 (-)^l R_n(\Omega_L - l\omega_f) \right|^2 \times \frac{1}{\sqrt{2\pi}\Delta_f} \exp\left(-\frac{\omega - \omega_f}{2\Delta_f}\right) \times P_n \quad (23)$$

Where P_n is the bimodal distribution, Ω_L is the laser excitation frequency, ω is the frequency of Stock range, Δ_f is the width of the Raman bands at ω_f , $S_{f,n}$ is the total Huang-Rhys factor and R_n is the function which related to zero and one-phonon process as well as the condition of conjugated bonding[168]. From this equation, it can be first found that the different conjugation length segments as difference lattice dynamic and vibration frequency. Secondly, RRS is also sensitive to the excitation frequency. The sensitivity of selective frequency gives characteristic to the segments of conjugation length [169]. If defects exist in the conjugated polymer, then it will create a decrease in the conjugation length and change the optical transition in polymer system. Furthermore, the scattering process is much faster than the optical transition, and then it will affect the absorption and intensity of RRS[170].

Conclusion

Successful optical characterizations of polymers require careful sample preparation, attention to experiment details, and cautious instrument handling. Optical characterizations are highly sensitive to impurities, thermal annealing history, method, and preparation. Five optical properties have been discussed in detail, namely, optical absorption, dispersion behavior, anisotropy, emission spectrum, and excitation spectrum. Modifications of polymeric materials result in different optical characteristics that are the fingerprints of a polymeric system.

Acknowledgment

This work was funded by The Fundamental Grant Scheme (FRGS) under the grant number 600-RMI/ST/FRGS 5/3/Fst(198/2010). The authors would like to thank fakultisainsgunaan, uitm and nanoscience Tech, Institutes of Science (IOS) for supporting this research.

References

- Chilton, J.A. and M.T. Goosey, *Special Polymers for Electronics and Optoelectronics*. 1995: Chapman & Hall.
- Shirakawa, H., et al., *Synthesis of electrically conducting organic polymers: halogen derivatives of polyacetylene, (CH)*. Journal of the Chemical Society, Chemical Communications, 1977. **0**(16): p. 578-580.
- Macdiarmid, A.G., *Synthetic metals: a novel role for organic polymers*. Synthetic Metals, 2001. **125**(1): p. 11-22.
- Heeger, A.J., *Nobel Lecture: Semiconducting and metallic polymers: The fourth generation of polymeric materials*. Reviews of Modern Physics, 2001. **73**(3): p. 681-700.
- Liu, L., et al., *Soliton propagation optimization and dynamic modulation in photonic crystal waveguide with polystyrene background*. Optics Communications, 2012. **285**(2): p. 171-177.
- Cardona, M., *Introduction*, in *Light Scattering in Solids I*. 1983, Springer Berlin Heidelberg. P. 1-22.
- Troger, F., et al., *Nonlinear Optics*, in *Springer Handbook of Lasers and Optics*. 2012, Springer Berlin Heidelberg. P. 161-251.
- Ward, I.M. and D.I. Bower, *Infrared dichroism, polarized fluorescence and Raman spectroscopy*, in *Structure and Properties of Oriented Polymers*. 1997, Springer Netherlands. P. 181-233.
- Xing, Y., et al., *Carbazole-pyrene-based organic emitters for electroluminescent device*. Chemical Physics Letters, 2005. **408**(1-3): p. 169-173.
- Tang, C.W. and S.A. vanslyke, *Organic electroluminescent diodes*, in *Applied Physics Letter*. 1987, AIP. P. 913-915.
- Burroughes, J.H., et al., *Light-emitting diodes based on conjugated polymers*. Nature, 1990. **347**: p. 539-541.
- Adachi, C., T. Tsutsui, and S. Saito, *Organic electroluminescent device having a hole conductor as an emitting layer*, in *Applied Physics Letter*. 1989, AIP. P. 1489-1491.
- Cho, Y.J. and J.Y. Lee, *Thermally stable aromatic amine derivative with symmetrically substituted double spirobifluorene core as a hole transport material for green phosphorescent organic light-emitting diodes*. Thin Solid Films, 2012. **522**(0): p. 415-419.
- Bejbouj, H., et al., *Influence of the nature of polyaniline-based hole-injecting layer on polymer light emitting diode performances*. Materials Science and Engineering: B, 2010. **166**(3): p. 185-189.
- Kim, S.Y., T. Noh, and S.-H. Lee, *High efficiency polymeric light-emitting diodes with a blocking layer*. Synthetic Metals, 2005. **153**(1-3): p. 229-232.
- Hagen, J.A., et al., *Enhanced emission efficiency in organic light-emitting diodes using deoxyribonucleic acid complex as an electron blocking layer*. Applied Physics Letters, 2006. **88**(17): p. 171109-171109-3.
- Sun, Q., et al., *Multilayer white polymer light-emitting diodes with deoxyribonucleic acid-cetyltrimethylammonium complex as a hole-transporting/ electron-blocking layer*. Applied Physics Letters, 2008. **92**(25): p. 251108-3.
- Madhwal, D., et al., *Increased luminance of MEH-PPV and PFO based LEDs by using salmon DNA as an electron blocking layer*. Journal of Luminescence, 2010. **130**(2): p. 331-333.
- Adachi, C., T. Tsutsui, and S. Saito, *Blue light-emitting organic electroluminescent devices*, in *Applied Physics Letter*. 1990, AIP. P. 799-801.
- Rouis, A., et al., *Transport mechanism and trap distribution in ITO/azo-calix[4]arene derivative/Al diode structure*. Physica B: Condensed Matter, 2007. **399**(2): p. 109-115.
- Zhao, J., et al., *Organic light-emitting diodes with AZO films as electrodes*. Synthetic Metals, 2000. **114**(3): p. 251-254.
- Adachi, C. And T. Tsutsui, *Molecular LED: Design and Concept of Molecular materials For High Performance OLED*, in *Organic Light Emitting Diode A Survey*, J. Shinar, Editor. 2004, Spinger-Verlag: New York.
- Geffroy, B., P. Le Roy, and C. Prat, *Organic light-emitting diode (OLED) technology: materials, devices and display technologies*. Polymer International, 2006. **55**(6): p. 572-582.
- Hung, L.S. and C.H. Chen, *Recent progress of molecular organic electroluminescent materials and devices*. Materials Science and Engineering: R: Reports, 2002. **39**(5-6): p. 143-222.
- Shun-Chi, C., et al., *Degradation mechanism of phosphorescent-dye-doped polymer light-emitting diodes*, in *Applied Physics Letter*. 2001, AIP. P. 2088-2090.

- Xiao, T., et al., *Fabrication and properties of hybrid polymer/small-molecular phosphorescent oleds based on poly(N-vinyl carbazole)*. Proceeding of SPIE, 2009. **7415**: p. 741521-1.
- Zhu, F., et al., *Optimized indium tin oxide contact for organic light emitting diode applications*. Thin Solid Films, 2000. **363**(1-2): p. 314-317.
- Gu, G., et al., *Transparent organic light emitting devices*. Applied Physics Letters, 1996. **68**(19): p. 2606-2608.
- Xu, D., et al., *An anode with aluminum doped on zinc oxide thin films for organic light emitting devices*. Physics Letters A, 2005. **346**(1-3): p. 148-152.
- Pei, Q., et al., *Polymer Light-Emitting Electrochemical Cells: In Situ Formation of a Light-Emitting p-n Junction*. Journal of the American Chemical Society, 1996. **118**(16): p. 3922-3929.
- Qibing Pei, et al., *Polymer Light-Emitting Electrochemical Cells* Science, 1995. **25** p. 1086-1088.
- Dick, D.J., et al., *Imaging the structure of the p-n junction in polymer light-emitting electrochemical cells*. Advanced Materials, 1996. **8**(12): p. 985-987.
- Dini, D., *Electrochemiluminescence from Organic Emitters*. Chemistry of Materials, 2005. **17**(8): p. 1933-1945.
- Manzanares, J.A., H. Reiss, and A.J. Heeger, *Polymer Light-Emitting Electrochemical Cells: A Theoretical Study of Junction Formation under Steady-State Conditions*. The Journal of Physical Chemistry B, 1998. **102**(22): p. 4327-4336.
- Alem, S. And J. Gao, *The effect of annealing/quenching on the performance of polymer light-emitting electrochemical cells*. Organic Electronics, 2008. **9**(3): p. 347-354.
- Matyba, P., M.R. Andersson, and L. Edman, *On the desired properties of a conjugated polymer-electrolyte blend in a light-emitting electrochemical cell*. Organic Electronics, 2008. **9**(5): p. 699-710.
- Demello, J.C., et al., *Ionic space-charge effects in polymer light-emitting diodes*. Physical Review B, 1998. **57**(20): p. 12951.
- Riess, I. And D. Cahen, *Analysis of light emitting polymer electrochemical cells*. Journal of Applied Physics, 1997. **82**(6): p. 3147-3151.
- Riess, I., *Polymeric mixed ionic electronic conductors*. Solid State Ionics, 2000. **136-137**: p. 1119-1130.
- Waldau, A.J., *PV Status Report 2003* 2003, European Commission. P. 20850 EN.
- Karsten, B.P., J.C. Bijleveld, and R.A.J. Janssen, *Diketopyrrolopyrroles as Acceptor Materials in Organic Photovoltaics*. Macromolecular Rapid Communications, 2010. **31**(17): p. 1554-1559.
- Pei, J., et al., *Efficiency enhancement of polymer solar cells by incorporating a self-assembled layer of silver nanodisks*. Solar Energy Materials and Solar Cells, 2011. **95**(12): p. 3281-3286.
- Liang, F., et al., *Donor-acceptor conjugates-functionalized zinc phthalocyanine: Towards broad absorption and application in organic solar cells*. Solar Energy Materials and Solar Cells, 2010. **94**(10): p. 1803-1808.
- Manceau, M., et al., *ITO-free flexible polymer solar cells: From small model devices to roll-to-roll processed large modules*. Organic Electronics, 2011. **12**(4): p. 566-574.
- Contreras, M.A., et al., *Progress toward 20% efficiency in Cu(In,Ga)Se₂ polycrystalline thin-film solar cells*. Progress in Photovoltaics: Research and Applications, 1999. **7**(4): p. 311-316.
- Xiang, X.B., et al., *The study on high efficient alxgal-xas/gaas solar cells*. Solar Energy Materials and Solar Cells, 2001. **68**(1): p. 97-103.
- Galiana, B., C. Algora, and I. Rey-Stolle, *Comparison of 1D and 3D analysis of the front contact influence on gaas concentrator solar cell performance*. Solar Energy Materials and Solar Cells, 2006. **90**(16): p. 2589-2604.
- Fang, Y.-Y., et al., *Molecular-Based Synthetic Approach to New Group IV Materials for High-Efficiency, Low-Cost Solar Cells and Si-Based Optoelectronics*. Journal of the American Chemical Society, 2008. **130**(47): p. 16095-16102.
- Reese, M.O., et al., *Consensus stability testing protocols for organic photovoltaic materials and devices*. Solar Energy Materials and Solar Cells, 2011. **95**(5): p. 1253-1267.
- Krebs, F.C., J. Fyenbo, and M. Jorgensen, *Product integration of compact roll-to-roll processed polymer solar cell modules: methods and manufacture using flexographic printing, slot-die coating and rotary screen printing*. Journal of Materials Chemistry, 2010. **20**(41): p. 8994-9001.
- Nozik, A.J., *Quantum dot solar cells*. Physica E: Low-dimensional Systems and Nanostructures, 2002. **14**(1-2): p. 115-120.
- O'Regan, B. And M. Grätzel, *A low-cost, high-efficiency solar cell based on dye-sensitized colloidal tio₂ films* Nature, 1991. **353**: p. 737-740.
- Yu, Z., et al., *Liquid electrolytes for dye-sensitized solar cells*. Dalton Transactions, 2011. **40**(40): p. 10289-10303.

- Kumar, U., et al., *Role of surface modification of colloidal cdse quantum dots on the properties of hybrid organic–inorganic nanocomposites*. Colloid and Polymer Science, 2010. **288**(8): p. 841-849.
- Wang, Z., et al., *Synthesis of MDMO-PPV capped pbs quantum dots and their application to solar cells*. Polymer, 2008. **49**(21): p. 4647-4651.
- Zhou, Y., et al., *Improved efficiency of hybrid solar cells based on non-ligand-exchanged cdse quantum dots and poly(3-hexylthiophene)*. Applied Physics Letters, 2010. **96**(1): p. 013304-3.
- Nozik, A.J., et al., *Semiconductor Quantum Dots and Quantum Dot Arrays and Applications of Multiple Exciton Generation to Third-Generation Photovoltaic Solar Cells*. Chemical Reviews, 2010. **110**(11): p. 6873-6890.
- Christian, G.D., *Analytical Chemistry, 6th Ed.* 2007: Wiley India Pvt. Limited.
- Perkampus, H.H., H.C. Grinter, and T.L. Threlfall, *UV-VIS Spectroscopy and Its Applications*. 2012: Springer London, Limited.
- Porro, T.J. and D.A. Terhaar, *Double-Beam Fluorescence Spectrophotometry*. Analytical Chemistry, 1976. **48**(13): p. 1103A-1107A.
- Robinson, J.W., E.M.S. Frame, and G.M. Frame, *Undergraduate Instrumental Analysis, Sixth Edition*. 2005: Marcel Dekker.
- Chen, S.B. and Z.Y. Zhong, *Optical and Dielectric Characteristics of Photoactive Layer Thin Films for Organic Photovoltaic Cells*. Applied Mechanics and Materials, 2012. **217 - 219**: p. 695-698.
- Schirmer, R.E., *Modern Methods of Pharmaceutical Analysis, Second Edition, Volume II*. 1991: Taylor & Francis Group.
- Aziz, N.D.A., R. Rusdi, and N. Kamarulzaman, *Studies of MEH-PPV and MEH-PPV/MCMB Films and their Light Absorption in the Red Wavelength Region of the Visible Spectrum*. Advanced Materials Research, 2012. **545**: p. 308-311.
- Tkacheno, N.V., *Optical Spectroscopy Methods and instrumentations*. 2006, Amsterdam Elsevier Publications.
- Skoog, D.A., F.J. Holler, and S.R. Crouch, *Principles of Instrumental Analysis*. 2007: Brooks/Cole. http://www.ssi.shimadzu.com/products/literature/Spectroscopy/UV-Vis_Accessories.pdf. 2013 5/3/2013].
- Bosch Ojeda, C. And F. Sanchez Rojas, *Recent developments in derivative ultraviolet/visible absorption spectrophotometry*. Analytica Chimica Acta, 2004. **518**(1–2): p. 1-24.
- Schroder, D.k., *Semiconductor Material and Device Characterization*. Third ed. 2006, New Jersey: John Wiley & Sons inc. <http://www.angstromadvanced.com/Products/phe101m.asp>. 2012 25/12/2012]. www.edmudoptic.com. 2012 21/12/2012].
- Tompkins, H.G., *Optical Components and the Simple PCSA (Polarizer, Compensator, Sample, Analyzer) Ellipsometer*, in *Handboo of Ellipsometry*, H.G. Tompkins and E.A. Irene, Editors. 2005, William Andrew, Inc.: New York.
- Fujiwara, H., *Principles of Spectroscopic Ellipsometry*, in *Spectroscopic Ellipsometry*. 2007, John Wiley & Sons, Ltd. P. 81-146.
- Sharma, K.K., *Optics Principles and Applications*. 2006, London: Academic Press.
- Pascu, R. And M. Dinescu, *Spectroscopy Ellipsometry*. Romanian Reports in Physics, 2012. **64**(1): p. 135-142.
- Azzam, R.M.A. and N.M. Bashara, *Ellipsometry and Polarized Light*. 1977, New York: Elsevier North-Holland.
- Fujiwara, H., *Spectroscopic Ellipsometry: Principles and Applications*. 2007: John Wiley & Sons.
- Froehlich, P.M. and G.G. Guilbault, *instrumentation For Fluorescence*, in *Practical Fluorescence: Edited by George G. Guilbault*, G.G. Guilbault, Editor. 1990, Dekker: New York.
- Hart, S.J. and R.D. jiji, *Light emitting diode excitation emission matrix fluorescence spectroscopy*. Analyst, 2002. **127**(12): p. 1693-1699.
- O'Connor, D.V. and D. Phillips, *Time-Correlated Single Photon Counting*. 1984, London: Academic Press.
- Klar, T.A., et al., *Fluorescence microscopy with diffraction resolution barrier broken by stimulated emission*. Proceedings of the National Academy of Sciences, 2000. **97**(15): p. 8206-8210.
- Weiss, S., *Shattering the diffraction limit of light: A revolution in fluorescence microscopy?* Proceedings of the National Academy of Sciences, 2000. **97**(16): p. 8747-8749.
- Sandoghdar, V., *Beating The Diffraction Limits*. Physics World, 2001(September): p. 29-33.
- Kaye, W., *Stray light ratio measurements*. Analytical Chemistry, 1981. **53**(14): p. 2201-2206.
- Lamb, W.E., Jr., *Anti-photon*. Applied Physics B, 1995. **60**(2-3): p. 77-84.
- Van Vleck, J.H. and D.L. Huber, *Absorption, emission, and linebreadths: A semihistorical perspective*. Reviews of Modern Physics, 1977. **49**(4): p. 939-959.
- Sze, S.M., *Physics of Semiconductor Devices*. 1981: Wiley.

- Larkin, P., *Infrared and Raman Spectroscopy; Principles and Spectral Interpretation*. 2011: Elsevier Science.
- Mccreery, R.L., *Raman Spectroscopy for Chemical Analysis*. Volume 225 of Chemical Analysis: A Series of Monographs on Analytical Chemistry and Its Applications. 2005, Canada: Wiley.
- Smith, E. And G. Dent, *Modern Raman Spectroscopy: A Practical Approach*. 2005: Wiley.
- Anderson, P.W., *Model for the Electronic Structure of Amorphous Semiconductors*. Physical Review Letters, 1975. **34**(15): p. 953-955.
- Mott, N.F. and E.A. Davis, *Conduction in non-crystalline systems*. Philosophical Magazine, 1968. **17**(150): p. 1269-1284.
- Wood, D.L. and J. Tauc, *Weak Absorption Tails in Amorphous Semiconductors*. Physical Review B, 1972. **5**(8): p. 3144-3151.
- Mott, N.F. and E.A. Davis, *Electronic Processes in Non-crystalline Materials*. 1971, London: Oxford University Press.
- Alias, A.N., et al., *Optical Characterization of Luminescence Polymer Blends Using Tauc/Davis-Mott Model*. Advanced Materials Research, 2012. **488-489**: p. 628-632.
- Tauc, J., *Optical Properties of Amorphous Semiconductor*, in *Amorphous and Liquid Semiconductor*, J. Tauc, Editor. 1973, Plenum Publishing Company LTD: London.
- Urbach, F., *The Long-Wavelength Edge of Photographic Sensitivity and of the Electronic Absorption of Solids*. Physical Review, 1953. **92**(5): p. 1324-1324.
- Dexter, D.L., *Interpretation of Urbach's Rule*. Physical Review Letters, 1967. **19**(24): p. 1383-1385.
- Redfield, D., *Effect of Defect Fields on the Optical Absorption Edge*. Physical Review, 1963. **130**(3): p. 916-918.
- Dow, J.D. and D. Redfield, *Toward a Unified Theory of Urbach's Rule and Exponential Absorption Edges*. Physical Review B, 1972. **5**(2): p. 594-610.
- Toyozawa, Y., *A Proposed Model For the Explanation of Urbach Edge*. Progress Theoretical Physics, 1959. **22**: p. 455-457.
- Skettrup, T., *Urbach's rule derived from thermal fluctuations in the band-gap energy*. Physical Review B, 1978. **18**(6): p. 2622-2631.
- Brazovskii, S.A., *Electronic Excitation in Peierls-Frohlich State*. Sov. Phys. JETP Lett, 1978. **28**: p. 606-610.
- Brazovskii, S.A. and Kirova N., *Exciton, Polarons and Bipolaron in Conducting Polymer*. Sov. Phys. JETP Lett, 1981. **33**: p. 4-8.
- Krishna, M.G. and A.K. Bhattacharya, *Effect of thickness on the optical absorption edge of sputtered vanadium oxide films*. Materials Science and Engineering: B, 1997. **49**(2): p. 166-171.
- Yakuphanoglu, F., M. Sekerci, and A. Balaban, *The effect of film thickness on the optical absorption edge and optical constants of the Cr(III) organic thin films*. Optical Materials, 2005. **27**(8): p. 1369-1372.
- Yahya, N.Z. and M. Rusop, *Investigation on the Optical and Surface Morphology of Conjugated Polymer MEH-PPV:zno Nanocomposite Thin Films*. Journal of Nanomaterials, 2012. **2012**: p. 4.
- Arslan, M., H. Duymusü, and F. Yakuphanoglu, *Optical Properties of the Poly(N-benzylaniline) Thin Film*. Journal Physic Chemistry, 2006. **110**: p. 276-280.
- Yahya, N.Z. and M. Rusop, *Optical and Structural Properties of MEH-PPV: zno Nanocomposites*. Advanced Materials Research, 2012. **364**: p. 124-128.
- Alias, A.N., et al., *Excitation and Emission Properties of Poly(N-carbazole)/Poly(vinylpyrrolidone) Blends Characterized By Fluorescence Spectroscopy*. Advanced Materials Research, 2013. **652-654**: p. 550-553.
- Alias, A.N., et al., *Optical Studies of poly (N-carbazole) (PVK) Blending With Polyvinylpyrrolidone (PVP) Using Tauc/Davis-Mott Model* Advanced Materials Research, 2013. **652-654**: p. 527-531.
- Alias, A.N., et al., *Optical Characterization of Thiophene Blending With Non-conjugated Polymer at Different Composition*. Advanced Materials Research, 2013. **600**: p. 15-18.
- Abdullah, O.G. and D.R. Saber, *Optical Absorption of Polyvinyl Alcohol Films Doped with Nickel Chloride*. Applied Mechanics and Materials, 2012. **110-116**: p. 177-182.
- Sadik, A.M., M.A. El-Morsy, and M.A. Shams-Eldin, *Interferometric testing and description of polarization ray tracing in multi-layer thin films*. Journal of Optics A: Pure and Applied Optics, 2008. **10**(11): p. 115003.
- Nasr, A.M., H.I. Abd El-Kader, and M. Farhat, *Characterization of photoactive polymer thin films using transmission spectrum*. Thin Solid Films, 2006. **515**(4): p. 1758-1762. Proceedings, 2012. **1482**(1): p. 667-672.
- Walton, A.K. and T.S. Moss, *Determination of Refractive Index and Correction to Effective Electron Mass in pbte and pbse*. Proceedings of the Physical Society, 1963. **81**(3): p. 509.
- Adachi, S., *Optical dispersion relations in amorphous semiconductors*. Physical Review B, 1991. **43**(15): p. 12316-12321.

- Penn, D.R., *Wave-Number-Dependent Dielectric Function of Semiconductors*. Physical Review, 1962. **128**(5): p. 2093-2097.
- Forouhi, A.R. and I. Bloomer, *Optical dispersion relations for amorphous semiconductors and amorphous dielectrics*. Physical Review B, 1986. **34**(10): p. 7018-7026.
- Forouhi, A.R. and I. Bloomer, *Optical properties of crystalline semiconductors and dielectrics*. Physical Review B, 1988. **38**(3): p. 1865-1874.
- Phillips, J.C., *Dielectric Definition of Electronegativity*. Physical Review Letters, 1968. **20**(11): p. 550-553.
- Ravindra, N.M., P. Ganapathy, and J. Choi, *Energy gap–refractive index relations in semiconductors – An overview*. Infrared Physics & Technology, 2007. **50**(1): p. 21-29.
- Wemple, S.H. and M. Didomenico, Jr., *Optical Dispersion and the Structure of Solids*. Physical Review Letters, 1969. **23**(20): p. 1156-1160.
- Wemple, S.H. and M. Didomenico, Jr., *Behavior of the Electronic Dielectric Constant in Covalent and Ionic Materials*. Physical Review B, 1971. **3**(4): p. 1338-1351.
- Yakuphanoglu, F., *Electrical conductivity, optical and metal–semiconductor contact properties of organic semiconductor based on MEH-PPV/fullerene blend*. Journal of Physics and Chemistry of Solids, 2008. **69**(4): p. 949-954.
- Alias, A.N., et al., *Refractive Index Dispersion and Optical Dielectric Properties Of Poly(N-carbazole)/Poly(vinylpyrrolidone) Blends*. Advanced Materials Research, 2013. **652-654**: p. 532-536.
- Abdelaziz, M., *Cerium (III) doping effects on optical and thermal properties of PVA films*. Physica B: Condensed Matter, 2011. **406**(6–7): p. 1300-1307.
- Dirix, Y., T.A. Tervoort, and C. Bastiaansen, *Optical properties of oriented polymer/dye polarizers*. Macromolecules, 1995. **28**(2): p. 486-491.
- Sharma, A. And S.G. Schulman, *Introduction of Fluorescence Spectroscopy*. 1999, New York: John Wiley.
- Thulstrup, E.W. and P.W. Thulstrup, *Polarization Spectroscopic Studies of Ordered Samples*. Acta Chimica Slovenica 2005. **52**(4): p. 371–383.
- Alias, A.N., et al. *Polarized Absorption and Dielectric Spectra of Poly (N-Carbazole) blends*. In 2012 IEEE Symposium on Business Engineering and Industrial Applications. 2012. Bandung.
- Alias, A.N., et al., *Characterization of Poly (N-vinylcarbazole) Blending with Different Composition By Using Polarized Electronic Spectroscopy*. Advanced Materials Research, 2013. **652-654**: p. 532-536.
- Lin, H.-W., et al., *Anisotropic optical properties and molecular orientation in vacuum-deposited ter(9,9-diarylfluorene)s thin films using spectroscopic ellipsometry*. Journal of Applied Physics, 2004. **95**(3): p. 881-886.
- Gaudin, O.P.M., et al., *Thickness dependent absorption spectra in conjugated polymers: Morphology or interference?* Applied Physics Letters, 2010. **96**(5): p. 053305.
- Koynov, K., et al., *Molecular weight dependence of birefringence of thin films of the conjugated polymer poly[2-methoxy-5-(2-[sup [prime]]-ethyl-hexyloxy)-1, 4-phenylenevinylene]*. Applied Physics Letters, 2004. **84**(19): p. 3792-3794.
- Tammer, M. And A.P. Monkman, *Measurement of the Anisotropic Refractive Indices of Spin Cast Thin Poly(2-methoxy-5-(2'-ethyl-hexyloxy)-p-phenylenevinylene) (MEH–PPV) Films*. Advanced Materials, 2002. **14**(3): p. 210-212.
- Jung, Y.W., et al., *Ellipsometric study on the optical property of UV exposed MEH-PPV polymer film*. Synthetic Metals, 2010. **160**(7–8): p. 651-654.
- Wasey, J.A.E., et al., *Effects of dipole orientation and birefringence on the optical emission from thin films*. Optics Communications, 2000. **183**(1–4): p. 109-121.
- Kasic, A., et al., *Free-carrier and phonon properties of n- and p-type hexagonal gan films measured by infrared ellipsometry*. Physical Review B, 2000. **62**(11): p. 7365-7377.
- Michelotti, F., et al., *Space charge effects in polymer-based light-emitting diodes studied by means of a polarization sensitive electroreflectance technique*. Journal of Applied Physics, 2002. **91**(9): p. 5521-5532.
- Schubert, M., et al., *Infrared ellipsometry characterization of conducting thin organic films*. Thin Solid Films, 2004. **455–456**: p. 295–300.
- Mauger, S.A. and A.J. Moule, *Characterization of new transparent organic electrode materials*. Organic Electronics, 2011. **12**(11): p. 1948-1956.
- Sole, J.G., L.E. Bausa, and D. Jaque, *An Introduction to the Optical Spectroscopy of Inorganic Solids*. 2005, West Sussex: John Wiley & Sons Ltd,

- Guilbault, G.G., *General Aspects of Luminescence Spectroscopy*, in *Practical Fluorescence: Edited by George G. Guilbault*, G.G. Guilbault, Editor. 1990, Dekker: New York.
- Heo, J., *Emission and local structure of rare-earth ions in chalcogenide glasses*. Journal of Non-Crystalline Solids, 2007. **353**(13–15): p. 1358-1363.
- Wang, R., et al., *Effect of optical basicity on Er³⁺ up-conversion luminescence in geo₂-R₂O glasses*. Journal of Non-Crystalline Solids, 2011. **357**(11–13): p. 2413-2416.
- Street, R.A., *Luminescence in Amorphous Semiconductors*. Advances in Physics, 1977. **24**(4): p. 397-454.
- Klick, C.C., *Experimentally Derived Configurational Coordinate Curves for Phosphors*. Physical Review, 1952. **85**(1): p. 154-155.
- Mott, N.F., *Photogeneration of Charge Carriers and Recombination in Amorphous Semiconductor*. Philosophical Magazine 1977. **36**(2): p. 413-420.
- Sprenger, D., *On the theory of absorption and luminescence spectra in amorphous semiconductors*. Physica status solidi (b), 1979. **94**(2): p. 583-593.
- Schwartz, B.J., *Conjugated Polymer As Molecular Materials: How Chain Conformation and Film Morphology Influence Energy Transfer and Interchain Interactions*. Annual Reviews Physic Chemistry, 2003. **54**: p. 141-172.
- Ton-That, C., M.R. Phillips, and T.-P. Nguyen, *Blue shift in the luminescence spectra of MEH-PPV films containing zno nanoparticles*. Journal of Luminescence, 2008. **128**(12): p. 2031-2034.
- Van Dijken, A., et al., *Influence of Adsorbed Oxygen on the Emission Properties of Nanocrystalline zno Particles*. The Journal of Physical Chemistry B, 2000. **104**(18): p. 4355-4360.
- Petrella, A., et al., *tio₂ nanocrystals – MEH-PPV composite thin films as photoactive material*. Thin Solid Films, 2004. **451–452**(0): p. 64-68.
- Yaliraki, S.N., *Theoretical Studies of Electronic and Nonlinear Optical Properties of Conjugated Polymer*, in *Department of Chemistry*. 1992, Massachusetts Institute of Techology.
- Cornil, J., et al., *Interchain Interactions in Organic π -Conjugated Materials: Impact on Electronic Structure, Optical Response, and Charge Transport*. Advanced Materials, 2001. **13**(14): p. 1053-1067.
- Orion, I., J.P. Buisson, and S. Lefrant, *Spectroscopic studies of polaronic and bipolaronic species in n-doped poly(paraphenylenevinylene)*. Physical Review B, 1998. **57**(12): p. 7050-7065.
- Rao, A.M., et al., *Infrared and Raman studies of pressure-polymerized C 60s*. Physical Review B, 1997. **55**(7): p. 4766-4773.
- Bree, A. And R. Zwarich, *Vibrational Assignment of Carbazole from Infrared, Raman, and Fluorescence Spectra*. The Journal of Chemical Physics, 1968. **49**(8): p. 3344-3355.
- Louarn, G., et al., *Vibrational Studies of a Series of .alpha.-Oligothiophenes as Model Systems of Polythiophene*. The Journal of Physical Chemistry, 1995. **99**(29): p. 11399-11404.
- Volz, C., M. Arif, and S. Guha, *Conformations in dioctyl substituted polyfluorene: A combined theoretical and experimental Raman scattering study*. The Journal of Chemical Physics, 2007. **126**(6): p. 064905-8.
- Carter, P.W. and J.D. Porter, *Probing of π conjugation in trans-polyacetylene using near-infrared photoluminescence spectroscopy*. Physical Review B, 1991. **43**(18): p. 14478-14487.
- Ehrenfreund, E., et al., *Amplitude and phase modes in trans-polyacetylene: Resonant Raman scattering and induced infrared activity*. Physical Review B, 1987. **36**(3): p. 1535-1553.
- Ariu, M., D.G. Lidzey, and D.D.C. Bradley, *Influence of film morphology on the vibrational spectra of dioctyl substituted polyfluorene (PFO)*. Synthetic Metals, 2000. **111–112**(0): p. 607-610.
- Ariu, M., et al., *A study of the different structural phases of the polymer poly(9,9'-dioctyl fluorene) using Raman spectroscopy*. Synthetic Metals, 2001. **116**(1–3): p. 217-221.
- Mulazzi, E., et al., *Theoretical and experimental investigation of absorption and Raman spectra of poly(paraphenylene vinylene)*. Physical Review B, 1999. **60**(24): p. 16519-16525.
- Brivio, G.P. and E. Mulazzi, *Theoretical analysis of absorption and resonant Raman scattering spectra of trans-(CH)_x*. Physical Review B, 1984. **30**(2): p. 876-882.
- Tiziani, R., G.P. Brivio, and E. Mulazzi, *Resonant Raman scattering spectra of trans-(CD)_x: Evidence for a distribution of conjugation lengths*. Physical Review B, 1985. **31**(6): p. 4015-4018.
- Surján, P.R. and H. Kuzmany, *Interruption of conjugations of polyacetylene chains*. Physical Review B, 1986. **33**(4): p. 2615-2624.